

1-1-2023

Discrimination between six commercially relevant and ecologically diverse fish species across the Gulf of Tunis using fatty acid composition and otolith shape analyses

NAWZET BOURIGA

WAFÄ RJİBA BÄHRİ

SAFA BEJÄOUI

MADEL F. ADJİBAYO HOUETO

ADEL A. BASYOUNY SHAHİN

See next page for additional authors

Follow this and additional works at: <https://journals.tubitak.gov.tr/zoology>



Part of the [Zoology Commons](#)

Recommended Citation

BOURIGA, NAWZET; BÄHRİ, WAFÄ RJİBA; BEJÄOUI, SAFA; HOUETO, MADEL F. ADJİBAYO; SHAHİN, ADEL A. BASYOUNY; QUİGANRD, JEAN-PIERRE; TRABELSI, MONIA; and FÄLEH, ABDERRÄOUF BEN (2023)

"Discrimination between six commercially relevant and ecologically diverse fish species across the Gulf of Tunis using fatty acid composition and otolith shape analyses," *Turkish Journal of Zoology*. Vol. 47: No. 4, Article 6. <https://doi.org/10.55730/1300-0179.3136>

Available at: <https://journals.tubitak.gov.tr/zoology/vol47/iss4/6>

This Article is brought to you for free and open access by TÜBİTAK Academic Journals. It has been accepted for inclusion in Turkish Journal of Zoology by an authorized editor of TÜBİTAK Academic Journals. For more information, please contact academic.publications@tubitak.gov.tr.

Discrimination between six commercially relevant and ecologically diverse fish species across the Gulf of Tunis using fatty acid composition and otolith shape analyses

Authors

NAWZET BOURIGA, WAFI RJIBA BAHRI, SAFA BEJAOUI, MADEL F. ADJIBAYO HOUETO, ADEL A. BASYOUNY SHAHIN, JEAN-PIERRE QUIGANRD, MONIA TRABELSI, and ABDERRAOUF BEN FALEH

Discrimination between six commercially relevant and ecologically diverse fish species across the Gulf of Tunis using fatty acid composition and otolith shape analyses

Nawzet BOURIGA^{1,2} , Wafa RJIBA BAHRI³ , Safa BÉJAOUÏ² , Madel F. ADJIBAYO HOUETO¹ ,

Adel A. BASYOUNY SHAHIN^{4,*} , Jean-Pierre QUIGANRD⁵ , Monia TRABELSI¹ , Abderraouf BEN FALEH¹ 

¹Laboratory of Ecology, Biology and Physiology of Aquatic Organisms (LR/18/ES/41), Faculty of Sciences of Tunis, University of Tunis El Manar, Tunis, Tunisia

²Higher Institute of Fisheries and Aquaculture of Bizerte, University of Carthage, Bizerte, Tunisia

³Laboratory of Biodiversity, Biotechnology and Climate Change (LR11ES09), Faculty of Sciences of Tunis, University Tunis El Manar, Tunis, Tunisia

⁴Department of Zoology, Faculty of Science, Minia University, El Minia, Egypt

⁵Laboratory of Ichthyology, University of Montpellier 2, Montpellier, France

Received: 03.04.2023

Accepted/Published Online: 22.06.2023

Final Version: 07.07.2023

Abstract: Fatty acid composition and otolith shape variation of six commercially important fishes, which differ ecologically in their living and feeding habits across the Gulf of Tunis, Tunisia, were analyzed. The aims were to investigate the discrimination and relationship between the six species using both fatty acid composition and otolith shape to examine whether variability in fatty acid composition is consistent with variation in otolith shape and check whether otoliths shape and fatty acids composition have combined characteristic signals for these species. Tukey's test with one-way ANOVA indicated significant differences in total percentages of saturated (SFAs), polyunsaturated (PUFAs), and monounsaturated (MUFAs) fatty acids between individuals of the six species, and only between males and females of *Gobius niger*, and *Trachinus draco*. Discriminant function analysis (DFA) separated the six species into two main distinct clusters or groups. The first group comprised *Mullus barbatus*, *G. niger*, and *T. draco*, which assume a benthic life, while the second included *Sardina pilchardus*, *Trachurus mediterraneus*, and *Chelon auratus*, which are benthopelagic to pelagic species. Wilk's λ test and Fisher's distance (D) matrix showed a significant bilateral asymmetry in the left and right otoliths shape between individuals of the six species, as well as only between males and females of *C. auratus*, *T. mediterraneus*, and *G. niger*. However, a significant bilateral asymmetry was found only between females of *G. niger* and males of *T. draco*. DFA and hierarchical ascending classification (HAC) based on otolith shape variance revealed two main groups of otoliths congruent to those obtained from fatty acid composition analysis. The results indicated that fatty acid composition analysis was compatible with otolith shape analysis, and both have combined characteristic signals for these species and validated the use of fatty acid composition and otolith shape analyses as an effective approach to discriminate between and within these species.

Key words: Benthic fishes, elliptical Fourier descriptors, fatty acid analysis, pelagic fishes, saccular otolith shape

1. Introduction

In Tunisian waters, six species, including the carangid Mediterranean horse mackerel *Trachurus mediterraneus*, sardine *Sardina pilchardus*, golden grey mullet *Chelon auratus*, red mullet *Mullus barbatus*, black goby *Gobius niger*, and greater weever *Trachinus draco* are common and represent the most important commercial fish species in the Gulf of Tunis located in north-eastern Tunisia. The distribution and feeding habits of these species are as follows: *T. mediterraneus* is a pelagic or benthopelagic, subtropical, and oceanodromous marine fish that feeds primarily on sardines, anchovies, and small crustaceans (Georgieva et al., 2019) and lives at depths up to 500 m

(usually 5 to 250 m) (FAO-FIGIS, 2005**). *S. pilchardus* is a small pelagic or sometimes benthopelagic species, highly opportunistic and flexible microphagous forager, often filter-feeding on native planktonic crustaceans (van der Lingen et al., 2009), and lives at depths of 10 to 100 m (Tous et al., 2015*). Similarly, *C. auratus* is a pelagic-neritic species that lives at depths of 10 to 20 m (Thomson, 1990). It typically lives ashore, entering lagoons, harbors, and estuaries but rarely moving into freshwater (Riede, 2004). However, it occasionally assumes a benthic nature and feeds on small benthic animals, debris, and, on rare occasions, insects, and plankton (Ben-Tuvia, 1986). *M. barbatus* is a benthic gregarious species (Özbilgin et al., 2004)

* Correspondence: adel.shahin@mu.edu.eg

but usually transitions between a pelagic and a demersal phase (Sonin et al., 2007). It inhabits on the continental shelf's sandy and muddy bottoms, with a wide distribution along the Mediterranean coasts (Özbilgin et al., 2004), and feeds on small invertebrates primarily Crustaceans, Polychaeta, Mollusca, Echinodermata, and small fishes that live on or within the bottom substrates (Toğulga, 1977). Although it prefers depths between 20 and 200 m, its habitat ranges from shallow littoral coasts to 300 m (Tserpes et al., 2002). *G. niger* has been classified as an omnivorous benthic species, feeding on a variety of invertebrates and occasionally small fish and inhabiting estuaries, coastal lagoons, and sea lochs up to 80 m deep, but most frequently between the surface and 30 m (Kara and Quignard, 2019). *T. draco* is a venomous benthic fish that lives most of its life on sandy or muddy bottoms at depths of 15 to 150 m (Roux, 1990), feeds mainly on small invertebrates and fish, and is primarily nocturnal (Morte et al., 1999).

So far, previous studies have demonstrated that the fatty acid composition varies widely among fish species depending on the feeding behavior and breeding strategies of each fish species (Zhang et al., 2020; Gonçalves et al., 2021). Therefore, the fatty acid composition has long been used as a chemotaxonomic marker for the identification and classification of fish species (Zhang et al., 2020; Gonçalves et al., 2021), as well as the assessment of environmental pollution (Zaoui et al., 2023). In animals, essential fatty acids (EFAs), especially eicosapentaenoic acid (EPA, C20:5n-3) and docosahexaenoic acid (DHA, C22:6n-3), play vital roles in reproduction, immune efficiency, osmoregulation, and arachidonic (ARA, C20:4n-6) activates the production of prostaglandins and leukotrienes (Bret and Müller-Navarra, 1997). Besides, both EPA and DHA are involved in the growth, development, and maintenance of brain structure and function (Horrocks and Akhlaq, 2004). In addition, along with its powerful impact on cognition and behavior, and protection against oxidative stress, DHA alone is crucial for the health, development of neurons, and neurotransmission (Kelly and Scheibling, 2012). Moreover, the nutritional quality index and the PUFA-n-6/n-3 ratio revealed that the consumption of PUFA-n-6 and n-3 can offer several benefits to human health, especially for those concerned with reducing the risks of cardiovascular diseases (Gonçalves et al., 2021). Therefore, the difference in feeding behavior, in terms of quality and quantity, among these abovementioned species would be expected to lead to differences in fatty acid profile.

Biologically, otoliths are calcified crystals of the inner ear used for balance and/or hearing in all teleosts and consist of a matrix of organic and inorganic components (Marmo, 1982). These otoliths are organized into three pairs, one pair of which, the sagittae, is the largest and most studied pair of otoliths in teleost fish. Previous studies have shown that saccular otoliths (sagittae) exhibit high inter-

and intraspecific variability in shape and size (D'Iglio et al., 2021; Yedier and Bostanci, 2021; Mejri et al., 2022a, 2022b; Yedier et al., 2023). Therefore, they have been used as an efficient tool to identify and classify fish species (Bostanci et al., 2015; Tuset et al., 2020; Mejri et al. 2022a) and populations (Bose et al., 2017; Bostanci and Yedier, 2018; Tuset et al., 2019; Carvalho et al., 2022), and to discriminate their stocks in different habitats (Trojette et al., 2015; Ben Labidi et al., 2020a; Khedher et al., 2021; Mahé et al., 2021; Mejri et al., 2022b). In addition, studies of morphological variability in the otolith shape, structure, and development have shown that the otolith shape is species-specific and its shape and size have been reported to reflect the species' living environment (Mille et al., 2015). These variabilities are influenced by ontogenetic, genetic, abiotic (e.g., temperature), and biotic (e.g., food availability; quantity, and quality) factors (Vignon and Morat, 2010; Ben Labidi et al., 2020a, 2020b; Khedher et al., 2021; Çöl and Yilmaz, 2022; Mejri et al., 2022a, 2022b), luminosity (Paxton, 2000), and depth at which fish live (Fashandi et al., 2019), as well as by sex, growth, and maturity (Begg and Brown, 2000; Yazici, 2023), or by individual genotype (Vignon and Morat, 2010) or physiological state (Campana and Neilson, 1985). Moreover, the shape of otoliths alone allowed not only to observe interspecific differences (Mejri et al., 2022a), but also intraspecific differences (Mahé et al., 2019; Ben Labidi et al., 2020a, 2020b; Khedher et al., 2021; Mejri et al., 2022b). Furthermore, it has been shown that variability in otolith shape is not an indicator of stress (Panfili et al., 2005) but a form of species adaptation to their living environments (Lychakov et al., 2008). Thus, morphological variability has been found in benthic fishes that live in aphotic areas where visual communication is difficult (Storelli et al., 1998).

Indeed, the discrepancy between the shape of the right and left otoliths has been expressed as bilateral asymmetry (BA) (Díaz-Gil et al., 2015; Jawad et al., 2023; Zhang et al., 2023). In addition, the deviation from perfect bilateral asymmetry has been attributed to either directional asymmetry (DA) (Mille et al., 2015; Mahé et al., 2021), antisymmetry (A) (Palmer and Strobeck, 1986; Govind and Pearce, 1986), or fluctuating asymmetry (FA) (Bostanci et al., 2018; Ben Labidi et al., 2020b; Khedher et al., 2021; Mejri et al., 2022b; Qasim et al., 2022; Yedier et al., 2022; Ben Mohamed et al., 2023). Although the various forms of otolith asymmetry have been reported in several fish species and have been attributed to developmental instability resulting from stress and environmental heterogeneity (Bostanci et al., 2018; Ben Labidi et al., 2020a, 2020b; Khedher et al., 2021; Mejri et al., 2022a, 2022b; Qasim et al., 2022; Yedier et al., 2022; Ben Mohamed et al., 2023), their origins and consequences remain still largely unclear and controversial. In addition, recent studies have shown that developmental instability has led to abnormalities of

otoliths' development (Yedier, 2022; Yedier et al., 2023) or the formation of anomalous or aberrant otoliths (Carvalho et al., 2019; Yedier and Bostanci, 2019, 2020; De Carvalho Lapuch et al., 2022).

Other studies have shown that the fat content of the fish diet or its biochemical composition and energy metabolism have been reported to influence otolith growth, structure, opacity, and shape (Mille et al., 2016). Moreover, Mahé et al. (2019) confirmed that eicosapentaenoic acid (EPA) and docosahexaenoic acid (DHA) are essential nutrients for most fish species and their deficiencies can affect many aspects of fish physiology, particularly the morphogenesis of otolith. Furthermore, Degens et al. (1969) indicated that dietary PUFA-n-3 could have a potential effect on the development of the audiovestibular system of fish, especially the biomineralization of otolith, which is based on a minor organic fraction accounting for 0.2 to 10% of the total material. On the other hand, Grønkjær (2016) described that the function of otoliths as a recorder of environmental signals is influenced by the physiology and genetic makeup of fish. Also, Yedier and Bostanci (2022), based on otolith shape and molecular (COI sequences) analyses, reported that otoliths possess phylogenetic signals for discrimination between the *Scorpaena* species. In addition, it has been inferred that the metabolic rate of fish controls the growth of both fish and otolith and leads to the observed proportionality between otoliths and fish size (Bang and Grønkjær, 2005). Physiologically, the process of growth ultimately involves the conversion of food contents into tissues, and proteins, amino acids, lipids, and other building blocks are transported into the blood to participate in the growth of the fish's organs and structures, including otoliths (Stanley et al., 2015). Likewise to the expectation that there would be differences in the fatty acid profile between these species under study due to the differences in their subsistence and feeding behavior, a difference in the shape of the otoliths would also be expected, and this difference might be consistent or compatible with differences in the fatty acid composition.

As far as known, the otolith approach has also been applied in studies related to ecological research and conservation applications (Miller et al., 2010), taxonomy and phylogeny (Béarez and Schwarzhans, 2013), evolution and ontogenetic processes (Capoccioni et al., 2011), spatiotemporal migrations (Smith and Kwak, 2014), and fish age (Škeljo et al., 2015), which have powerful implications for fisheries science and management (Vasconcelos et al., 2018). In addition, several methods have recently combined both morphometric or molecular and otolith biometry to differentiate and address the phylogenetic relationships between and within species (Yedier and Bostanci, 2021, 2022).

Among the aforementioned species, otolith characteristics have been investigated in *S. pilchardus* and *Engraulis encrasicolus* (Khemiri et al., 2014), *T. draco* (Fatnassi et al., 2017), and *M. barbatus* (Bakkari et al., 2020), while reproductive biology and diet composition have only been described in *T. draco* (Fatnassi et al., 2017), *G. niger* (Joyeux et al., 1991a, 1991b), and *T. mediterraneus* (Georgieva et al., 2019). In addition, these six species have been categorized into two groups based on the variation in otolith mass asymmetry (X): pelagic, including *S. pilchardus*, *T. mediterraneus*, and *C. auratus*, and benthic, which comprised *G. niger*, *M. barbatus*, and *T. draco* (Bouriga et al., 2021).

Despite these studies, no work has been carried out combining both otolith shape and fatty acid composition analyses to discriminate between fish species either in Tunisian waters or elsewhere. Therefore, the present study was conducted for the first time to (i) investigate the discrimination and relationship between the six species using both otolith shape and fatty acid composition, (ii) examine whether the variation in fatty acid composition is consistent or compatible with the difference in otolith shape, and (iii) check whether the otoliths shape and fatty acids composition have combined characteristic signals for these species.

2. Materials and methods

2.1. Sampling and study area

A total of 403 adult males (♂) and females (♀) of *C. auratus*, *T. mediterraneus*, *S. pilchardus*, *M. barbatus*, *G. niger*, and *T. draco* were collected between March and May 2017 from five marine stations located in the Gulf of Tunis using artisanal fishing (Figure 1). These stations and their geographical coordinates are La Goulette (36°49'09"N, 10°18'36"E), Southern Lake of Tunis (36°49'03"N, 10°14'33"E), Rades (36°46'30"N, 10°17'30"E), Hammam-Lif (36°44'13"N, 10°20'00"E), and Soliman (36°43'10"N, 10°24'00"E). Immediately after catching, individuals were examined visually for sexual maturity, or microscopically in the case of small gonads, to confirm the maturity of all individuals of the six species. In addition, the total length (TL) was measured with an ichthyometer to the nearest 0.1 cm, and the total weight (TW) was calculated with a digital balance to the nearest 0.1 g for both males and females of each species (Table 1).

2.2. Lipid extraction

Crude fats were extracted using chloroform: methanol (2:1) and the lipid fraction was determined gravimetrically. All values were expressed as the mean percentage of wet weight (ww) for the three replicates.

2.3. Fatty acid determination

Fatty acid methyl esters (FAMES) of fresh fillets from all individuals of the six species were determined in triplicate by the method of Lepage and Roy (1984). Briefly, the

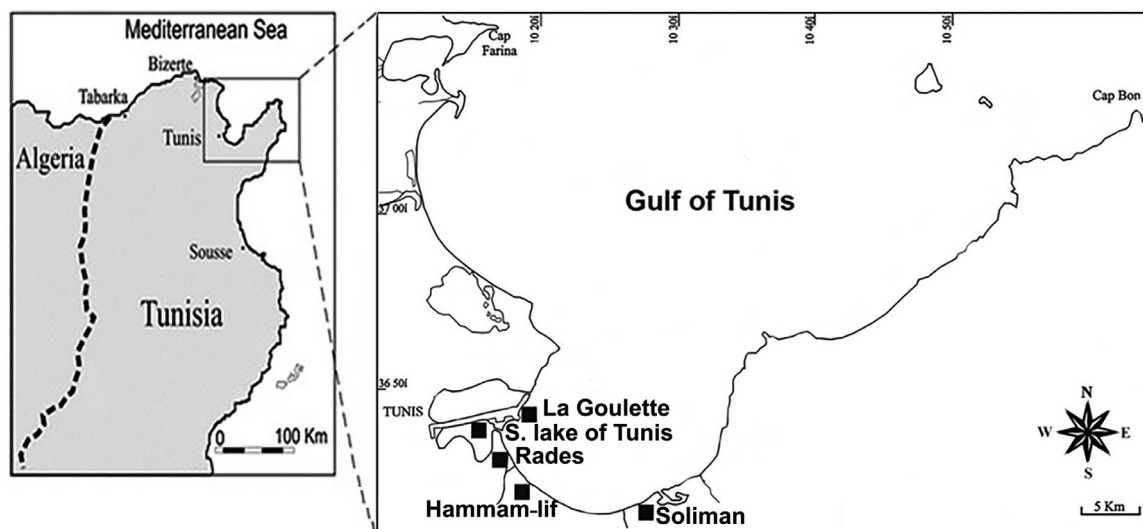


Figure 1. Study area and location of the sampling stations (■) from which individuals of the six species were collected from the Gulf of Tunis, Tunisia.

Table 1. The number (n), total weight (TW in g) and length (TL in cm), and mean \pm standard deviation (SD) of males (♂) and females (♀) examined from the six species collected from the five stations in the Gulf of Tunis, Tunisia.

Species (n)	Sex (n)	Range of TW (mean \pm SD)	Range of TL (mean \pm SD)
<i>C. auratus</i> (60)	♂ (30)	13–32 (26.8 \pm 3.2)	11–23 (17 \pm 7.2)
	♀ (30)	13–32 (27.1 \pm 3.2)	11–23 (17.2 \pm 7.2)
<i>T. mediterraneus</i> (73)	♂ (43)	17–49 (37.1 \pm 9.9)	8–18 (13 \pm 1.9)
	♀ (30)	17–49 (38.1 \pm 9.9)	8–18 (12.3 \pm 1.9)
<i>S. pilchardus</i> (66)	♂ (36)	5–14 (9.98 \pm 3)	4–16 (10 \pm 3)
	♀ (30)	5–14 (10.8 \pm 3)	4–16 (9.5 \pm 3)
<i>G. niger</i> (77)	♂ (45)	8–22 (18.1 \pm 5.4)	5–18 (11.5 \pm 1.6)
	♀ (32)	8–22 (20.0 \pm 5.4)	5–18 (10.3 \pm 1.6)
<i>T. draco</i> (60)	♂ (30)	24–38 (36.1 \pm 5.6)	11.5–20.5 (16 \pm 5)
	♀ (30)	24–38 (37 \pm 5.6)	11.5–20.5 (15 \pm 5)
<i>M. barbatus</i> (67)	♂ (30)	11–42 (39.4 \pm 8.1)	7–16 (11.5 \pm 2.2)
	♀ (37)	11–42 (40.4 \pm 8.1)	7–16 (11.9 \pm 2.2)

analysis was performed on a Varian Agilent 6890N gas chromatograph, which was equipped with an automatic sampler and equipped with split/splitless injectors, and a flame ionization detector (FID). The separation was performed in an Innowax 30 \times 0.25 capillary column (25 m \times 0.25 mm ID, film thickness). The temperature was programmed from 180 to 200 $^{\circ}$ C at 4 $^{\circ}$ C/min, held at 200 $^{\circ}$ C for 10 min, heated to 210 $^{\circ}$ C at 4 $^{\circ}$ C/min, and held at 210 $^{\circ}$ C for 14.5 min using an injector and FID at 250 $^{\circ}$ C. The fatty acid content in the total lipids of the samples was estimated using henicosaic acid C21:0, as an internal standard (10 mg/mL) based on the peak area ratio. The sequences of

fatty acid were ranged according to the chromatographic retention times, and the values are given as percentages of the total fatty acid methyl esters for three replicates.

2.4. Otolith extraction

Left and right otoliths were extracted from all individuals of the six species and then, the otoliths were cleaned with distilled water, stored in Eppendorf tubes, and kept in dry storage for 24 h to eliminate humidity.

2.5. Otolith shape analysis

Each otolith was placed on a microscope slide on its convex side with the sulcus pointing down and the rostrum

pointing in the same direction to minimize distortion errors in the normalization process. Subsequently, as shown in Figure 2, each pair of otoliths was photographed under the binocular loupe using a 20 megapixels Canon Ixus 185 high-performance digital camera to obtain images that allow us to trace the outlines of the shape with perfect accuracy. The obtained images were then processed by Photoshop CS6 software, which transformed the original images of otoliths into binary images. Afterwards, images of the shapes were analyzed using Shape 1.3 software (Iwata and Ukai, 2002). The contour shape of each otolith was evaluated by elliptical Fourier analysis (EFA) as previously described by Ben Labidi et al. (2020a, 2020b). In the method of elliptical Fourier descriptors (EFDs), the chain-coding algorithm was used and calculated based on the projection of the binary contour of each otolith using Shape 1.3 software. The chain-coder provided the normalized EFDs coefficients through the discrete Fourier transformation (DFT) of the chain-coded contour. The EFDs technique described the outline based on the harmonics and generated 20 harmonics for each otolith. Each harmonic consists of four coefficients (A, B, C, and D), which corresponded to the sine and cosine values of the variation in the x and y coordinates and resulted in 80 coefficients per otolith produced by projecting each point of the outline onto the (x) and (y) axes. The four Fourier descriptors (FDs) were normalized using the first harmonic to make them

invariant with changes in size, location, rotation, and starting point. After transformation, the first three FDs of the first harmonic were fixed to constant values and were therefore not considered in the analysis. Therefore, each sample was represented by the subsequent 77 coefficients. To determine the number of harmonics required to reconstruct the best otolith outline, the cumulated Fourier power (FP_n) was calculated for each otolith as a measure of the precision of contour reconstruction obtained using the n harmonics, i.e. the proportion of variance in the contour coordinates computed by the n harmonics. The Fourier power (FP_n), the Fourier power percentage (FP%), and the cumulative Fourier power percentage ($FP_n\%$ cumulative) were calculated according to the following formulae:

The Fourier power

$$PF_n = \frac{A_n^2 + B_n^2 + C_n^2 + D_n^2}{2},$$

where A_n , B_n , C_n , and D_n are the Fourier coefficients of the n harmonics.

The Fourier power percentage

$$PF\% = \left(PF_n / \sum_1^n PF_n \right) \times (100)$$

The cumulative Fourier power percentage

$$PF_n\%c = \sum_1^n PF_n^0 / 0$$

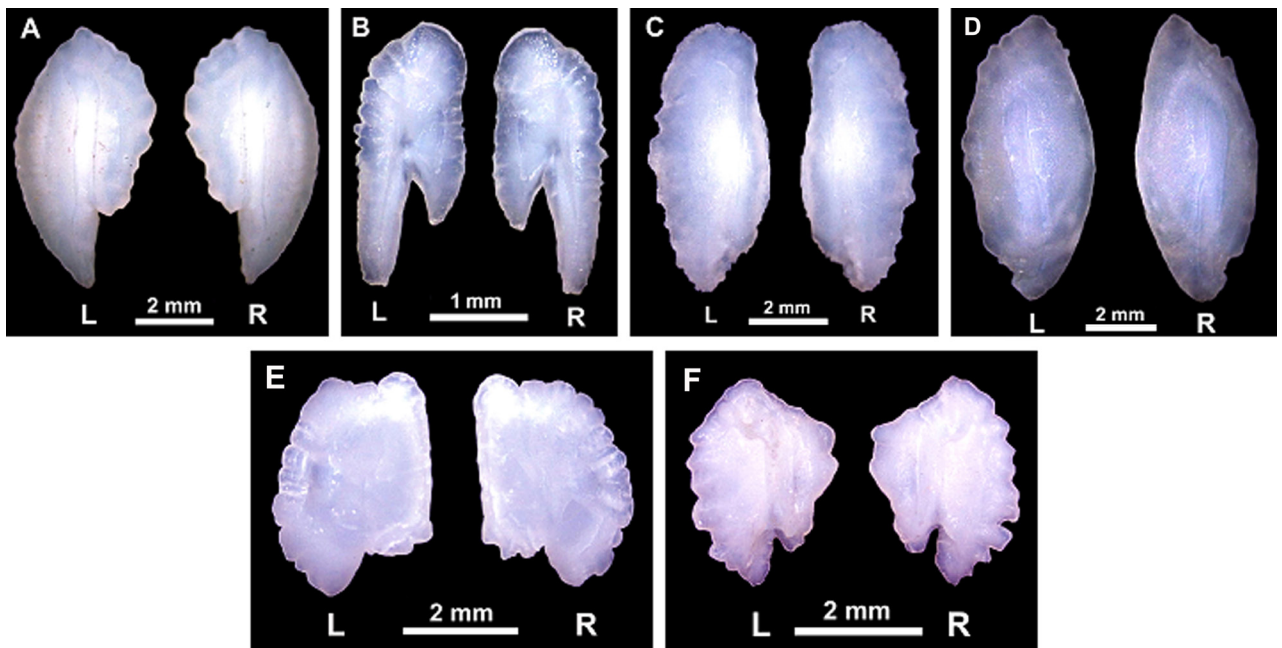


Figure 2. Real images of the left (L) and right (R) otoliths of (A) *T. mediterraneus*, (B) *S. pilchardus*, (C) *C. auratus*, (D) *T. draco*, (E) *G. niger*, and (F) *M. barbatus* individuals collected from the five stations in the Gulf of Tunisia, Tunisia.

The FP_n was calculated for each otolith to ensure that each otolith in the sample was reconstructed with a precision of 99.99%, and the total FP_n was calculated to determine the number of harmonics required. The maximum number of harmonics $n = \max(n)$ across all otoliths was then used to reconstruct each otolith.

2.6. Statistical analysis

2.6.1. Fatty acids analysis

Statistical analysis of fatty acid composition and sequence values was performed in triplicates using SAS software (SAS 9.1.3, 2002-2003, Institute Inc., Cary, NC, USA). The comparison of fatty acid composition at the inter- and intraspecific levels, i.e. among and within males and females, was tested using the 5% Tukey's test with a one-way analysis of variance (ANOVA). In addition, differences in fatty acid composition at the inter- and intraspecific levels were detected using discriminant function analysis (DFA) and principal component analysis (PCA), respectively.

2.6.2. Otolith shape analysis

Differences in the contour shape of the left and right otoliths at the inter- and intraspecific levels of the six species were revealed using discriminant function analysis (DFA). The effect of species on elliptical Fourier descriptors was first tested by multivariate analysis of variance (MANOVA). First, all shape variable values were checked for being normal, and if the values did not follow a normal distribution, a Box-Cox transformation was performed. Second, Levene's and Shapiro-Wilk's λ tests were applied to assess homogeneity (equality) and normality of variance in the variable values of otolith shapes, respectively. Afterwards, DFA was performed using the normalized elliptical Fourier descriptors coefficients (77 coefficients per otolith) to illustrate the similarities and differences at the inter- and intraspecific levels of the six species. The objective of the DFA is to investigate the integrity of predetermined groups of individuals of a particular species and the percentage of their correct classification, by finding linear combinations of descriptors that maximize Wilk's λ value. Wilk's λ test evaluates the performance of discriminant analyses. This statistic is the ratio between intraspecific variance and total variance and provides an objective method for calculating the corrected percentage chance of agreement. In addition, Fisher's distance (D) was also calculated to describe the differences in the shape of otolith at the inter- and intraspecific levels. Moreover, a hierarchical ascending classification (HAC) analysis was performed based on the values of the otoliths' shapes divergence between the six species. Furthermore, PCA was performed to assess the consistency between the fatty acid composition and otolith shape among individuals of the six species. All statistical analyses were performed

using XLSTAT 2010. The results were interpreted using data from Wilk's λ test, and the barycenter projections for the left and right otoliths of both males and females for each of the six species were shown on graphs. In addition, the MANOVA was used to test the significance of the left and right otoliths' shape values between and within species.

3. Results

3.1. Total weight (TW) and total length (TL) variation

As shown in Table 1, the body weight (TW) and total length (TL) of males and females in the benthic species ranged from 11 to 42 g and 7 to 16 cm in *M. barbatus*, from 8 to 22 g and 5 to 18 cm in *G. niger*, and from 24 to 38 g and 11.5 to 20.5 cm in *T. draco*, respectively. In the pelagic *C. auratus*, the TW varied from 13 and 32 g and the TL differed from 11 to 23 cm in both males and females, respectively. However, in the pelagic or benthopelagic *T. mediterraneus* and *S. pilchardus*, the TW and TL ranged from 17 to 49 g and 8 to 18 cm, and 5 to 14 g and 4 to 16 cm in both males and females, respectively.

3.2. Fatty acids composition variation

At the interspecific level, Tukey's 5% test with one-way ANOVA detected a significant difference ($p < 0.0001$) in the total percentages of both saturated fatty acids (SFAs), polyunsaturated fatty acids (PUFAs), and monounsaturated fatty acids (MUFAs) between individuals of the six species (Table 2). Polyunsaturated fatty acids (PUFAs) were more abundant in *T. mediterraneus*, *S. pilchardus*, and *C. auratus* ($47.25 \pm 1.92\%$) than in *M. barbatus*, *G. niger*, and *T. draco* ($31 \pm 1.86\%$). Among the SFAs, the contents of palmitic acid (C16:0) and stearic acid (C18:0) were the most predominant fatty acids for the six species and the content of C16:0 was significantly higher ($p < 0.0001$) in *M. barbatus*, *G. niger*, and *T. draco* than in *T. mediterraneus*, *S. pilchardus*, and *C. auratus*. In addition, the most abundant MUFAs were oleic acid (C18:1), which accounted for $14.71 \pm 2.5\%$ among *T. mediterraneus*, *S. pilchardus*, and *C. auratus* and $5.63 \pm 0.75\%$ among *M. barbatus*, *G. niger*, and *T. draco*. Moreover, the contents of PUFAs in all species were dominated by essential fatty acids, such as eicosapentaenoic fatty acid (EPA), docosahexaenoic fatty acid (DHA), and arachidonic fatty acid (ARA), which differed in their content between $2.57 \pm 0.58\%$ and $29.96 \pm 2.08\%$ among the six species (Table 1). Of these essential PUFAs, DHA was the most abundant among the six species, followed by EPA and ARA, respectively. DHA alone accounted for more than 50% ($29.96 \pm 2.08\%$) of the total PUFAs content in *T. mediterraneus*, *S. pilchardus*, and *C. auratus* compared to only $13.07 \pm 0.44\%$ in *M. barbatus*, *G. niger*, and *T. draco*. Furthermore, the highest amounts of PUFA-3 and -6 were found in *T. mediterraneus*, *S. pilchardus*, and *C. auratus* ($39.58 \pm 2.25\%$ and $4.79 \pm 0.5\%$, respectively), which significantly exceeded those found in *M. barbatus*, *G. niger*, and *T. draco* ($25.18 \pm 1.49\%$ and $2.89 \pm 0.45\%$, respectively).

Table 2. Mean and standard deviation (\pm SD) percentage (%) of fatty acids composition between individuals of the six species collected from the five stations in the Gulf of Tunis, Tunisia.

Fatty acid	Mean of total fatty acids (mg/mL) \pm SD (%)						Significance/ p-value
	<i>C. auratus</i>	<i>T. mediterraneus</i>	<i>S. pilchardus</i>	<i>G. niger</i>	<i>T. draco</i>	<i>M. barbatus</i>	
C12:0	0.14 \pm 0.01	0.2 \pm 0.03	0.44 \pm 0.17	0.19 \pm 0.02	0.44 \pm 0.26	0.12 \pm 0.01	NS
C14:0	5.56 \pm 0.39 ^a	2.28 \pm 0.17 ^c	2.70 \pm 1.08 ^{bc}	2.71 \pm 0.21 ^{bc}	3.94 \pm 0.24 ^b	3.33 \pm 0.01 ^{bc}	0.0016
C15:0	0.35 \pm 0.02 ^{bc}	0.51 \pm 0.04 ^{ab}	0.65 \pm 0.24 ^a	0.1 \pm 0.01 ^c	0.22 \pm 0.08 ^{bc}	0.36 \pm 0.08 ^{abc}	0.0195
C16:0	22.16 \pm 0.79 ^d	22.6 \pm 10.52 ^d	24.98 \pm 0.88 ^c	29.58 \pm 0.34 ^{ab}	31.04 \pm 0.88 ^a	28.99 \pm 0.12 ^b	< 0.0001
C17:0	0.12 \pm 0.00 ^d	0.6 \pm 0.04 ^{ab}	0.34 \pm 0.1 ^{dc}	0.72 \pm 0.01 ^a	0.72 \pm 0.16 ^a	0.45 \pm 0.14 ^{bc}	0.0019
C18:0	8.25 \pm 0.07 ^a	8.24 \pm 0.26 ^a	6.52 \pm 0.33 ^c	7.37 \pm 0.0 ^b	7.37 \pm 0.06 ^b	7.11 \pm 0.36 ^{bc}	0.0003
C20:0	0.21 \pm 0.05 ^b	0.17 \pm 0.02 ^b	0.16 \pm 0.04 ^b	0.66 \pm 0.03 ^a	0.15 \pm 0.06 ^b	0.83 \pm 0.36 ^a	0.0086
C22:0	0.54 \pm 0.10 ^a	0.34 \pm 0.01 ^b	0.2 \pm 0.07 ^{bc}	0.1 \pm 0.01 ^c	0.14 \pm 0.03 ^c	0.36 \pm 0.11 ^b	0.0019
C24:0	1.2 \pm 0.05 ^a	0.59 \pm 0.09 ^b	0.21 \pm 0.14 ^c	1.26 \pm 0.03 ^a	1.34 \pm 0.13 ^a	1.32 \pm 0.09 ^a	< 0.0001
Σ SFAs	38.55 \pm 0.21^b	35.56 \pm 0.32^b	36.22 \pm 1.98^b	42.69 \pm 0.12^a	45.37 \pm 1.57^a	42.88 \pm 0.09^a	< 0.0001
C16:1	2.06 \pm 0.05 ^b	2.31 \pm 0.23 ^b	2.23 \pm 0.27 ^b	4.29 \pm 0.05 ^a	4.19 \pm 0.2 ^a	4.45 \pm 0.12 ^a	< 0.0001
C17:1	0.22 \pm 0.01 ^b	0.25 \pm 0.01 ^b	0.16 \pm 0.04 ^b	0.1 \pm 0.01 ^b	0.19 \pm 0.01 ^b	0.67 \pm 0.24 ^a	0.0074
C18:1	14.37 \pm 0.01 ^b	11.49 \pm 0.1 ^c	18.28 \pm 0.85 ^a	5.01 \pm 0.03 ^c	5.17 \pm 0.42 ^c	6.7 \pm 0.19 ^d	< 0.0001
C20:1	5.71 \pm 0.04	0.71 \pm 0.18	0.25 \pm 0.06	1.79 \pm 0.01	1.93 \pm 0.02	1.89 \pm 0.03	NS
C22:1	0.28 \pm 0.59	0.07 \pm 0.03	0.54 \pm 0.28	0.18 \pm 0.03	0.25 \pm 0.09	0.22 \pm 0.01	NS
C24:1	0.47 \pm 3.72 ^b	0.94 \pm 0.03 ^a	0.7 \pm 0.27 ^{ab}	0.02 \pm 0.01 ^c	0.58 \pm 0.12 ^{ab}	0.34 \pm 0.11 ^c	0.0066
Σ MUFAs	23.13 \pm 0.05^a	15.79 \pm 0.32^b	22.18 \pm 0.01^a	11.39 \pm 0.05^c	12.32 \pm 0.58^c	14.27 \pm 0.19^{bc}	< 0.0001
C18:2	2.6 \pm 0.03 ^{ab}	2.73 \pm 0.03 ^{ab}	1.89 \pm 0.29 ^{bc}	1.36 \pm 0.01 ^c	3.3 \pm 0.64 ^a	2.55 \pm 0.35 ^{ab}	0.0054
C20:2	0.26 \pm 0.20 ^c	0.32 \pm 0.08 ^c	0.86 \pm 0.24 ^a	0.42 \pm 0.04 ^{bc}	0.66 \pm 0.07 ^{ab}	0.5 \pm 0.09 ^{bc}	0.0122
C18:3	1.98 \pm 0.06 ^c	1.37 \pm 0.09 ^d	1.43 \pm 0.05 ^d	2.18 \pm 0.15 ^c	2.61 \pm 0.01 ^b	3.29 \pm 0.01 ^a	< 0.0001
C20:3n-3	0.07 \pm 0.07 ^c	0.03 \pm 0.02 ^c	0.22 \pm 0.0 ^c	1.89 \pm 0.11 ^b	2.09 \pm 0.03 ^b	2.6 \pm 0.29 ^a	< 0.0001
C20:3n-6	0.12 \pm 0.19 ^c	0.15 \pm 0.02 ^c	0.46 \pm 0.04 ^b	0.1 \pm 0.01 ^c	0.16 \pm 0.04 ^c	0.64 \pm 0.09 ^a	< 0.0001
C18:4n-3	0.15 \pm 0.02	0.13 \pm 0.04	0.33 \pm 0.16	0.1 \pm 0.01	0.3 \pm 0.13	0.34 \pm 0.15	NS
C20:4n-6 (ARA)	4.4 \pm 0.001 ^a	3.93 \pm 0.34 ^{ab}	4.98 \pm 0.4 ^a	3.21 \pm 0.13 ^{bc}	2.64 \pm 0.02 ^{cd}	1.84 \pm 0.78 ^d	0.0003
C22:4n-6	0.23 \pm 0.001 ^a	0.03 \pm 0.01 ^b	0.02 \pm 0.0 ^b	0.01 \pm 0.001 ^b	0.03 \pm 0.01 ^b	0.01 \pm 0.0 ^b	< 0.0001
C20:5n-3 (EPA)	7.2 \pm 0.18 ^a	7.0 \pm 0.55 ^a	6.17 \pm 0.03 ^b	5.78 \pm 0.15 ^b	6.08 \pm 0.03 ^b	6.86 \pm 0.2 ^a	0.0030
C22:5n-3	0.8 \pm 0.03 ^{ab}	1.32 \pm 0.02 ^a	0.62 \pm 0.4 ^{bc}	0.12 \pm 0.01 ^c	0.77 \pm 0.41 ^{abc}	1.26 \pm 0.1 ^{ab}	0.0206
C22:6n-3 (DHA)	28.9 \pm 0.15 ^b	33.08 \pm 0.35 ^a	27.89 \pm 0.32 ^c	13.5 \pm 0.05 ^d	12.86 \pm 0.22 ^d	12.84 \pm 0.53 ^d	< 0.0001
Σ PUFAs	46.73 \pm 1.33^b	50.13 \pm 1.04^a	44.89 \pm 0.26^b	28.69 \pm 0.25^d	31.53 \pm 1.34^c	32.76 \pm 0.27^c	< 0.0001
Σ PUFAs-n-3	39.11 \pm 0.07^b	42.95 \pm 0.37^a	36.67 \pm 0.37^c	23.58 \pm 0.13^c	24.73 \pm 0.08^e	27.21 \pm 0.68^d	< 0.0001
Σ PUFAs-n-6	4.76 \pm 2.87^{ab}	4.12 \pm 0.77^{bc}	5.47 \pm 0.16^a	3.32 \pm 0.17^{dc}	2.84 \pm 0.69^d	2.5 \pm 0.67^d	0.0001

Abbreviation: ^{a-c}, differences between the six species, with the same letter within the same line, are not significantly different, ($p > 0.05$); NS: not significant; SFAs: saturated fatty acids; MUFAs: monounsaturated fatty acids; PUFAs: polyunsaturated fatty acids; EPA: eicosapentaenoic fatty acid; DHA: docosahexaenoic fatty acid; ARA: arachidonic fatty acid.

Moreover, as shown in Figure 3a, the barycenter projection based on DFA of the differences in fatty acid composition between individuals showed that the six species were discriminated from each other by the F1 and F2 axes, with a total variance value equal to 99.93%. Of these two axes, the F1

axis accounted for 80.71% of the total variation and placed *C. auratus*, *S. pilchardus*, and *T. mediterraneus* in the positive part and *M. barbatus*, *G. niger*, and *T. draco* in the negative part. However, the F2 axis explained 19.22% of the total variance and segregated *C. auratus*, *S. pilchardus*,

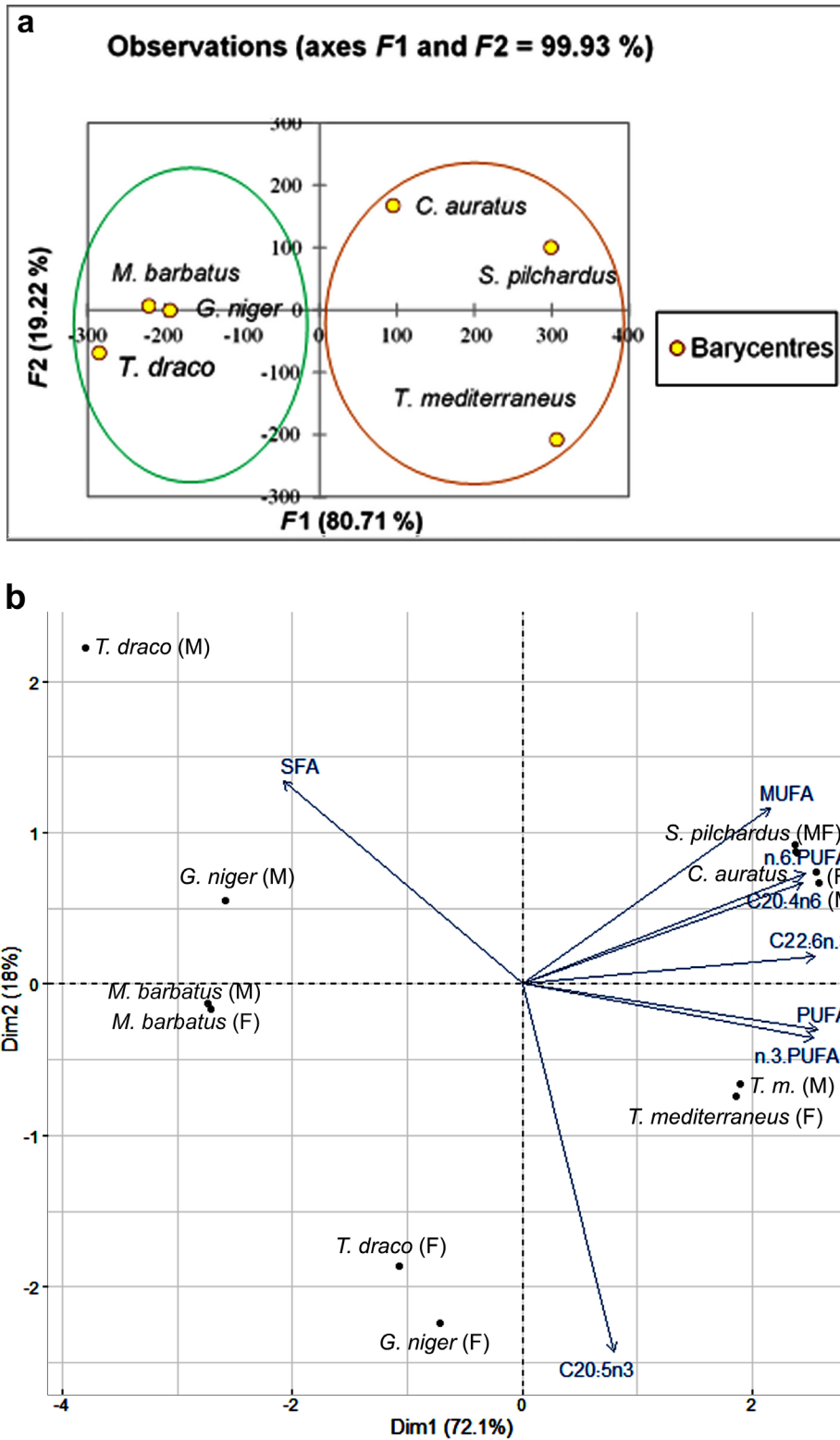


Figure 3. (a) Discriminant function analysis (DFA) and (b) principal component analysis (PCA) graph (biplot) showing the barycenter projection and distribution of the fatty acid composition percentage values between and within males (M) and females (F) of the six species collected from the five stations in the Gulf of Tunis, Tunisia. *T.m.*: *T. mediterraneus*.

and *M. barbatus* in the positive part and *T. draco*, *G. niger*, and *T. mediterraneus* in the negative. Therefore, as shown in Table 1, we can assume that the F1 axis was associated with the highest levels of MUFAs and PUFAs, especially DHA—22:6n-3, EPA—20:5n-3, ARA—20:4n-6, and PUFA-3 and -6, while the F2 axis was associated with the highest C18:3n-3, C20:3n-3, and SFAs, especially C16:0, C17:0, C20:0, and C24:0.

At the intraspecific level, significant differences between males and females were found in MUFA-C16:1 (palmitoleic acid) and C17:1 (ginkgolic acid), and PUFA-C22:5n-3 (Docosapentaenoic acid, DPA) in *C. auratus*, SFA-C12:0 (duodecylic acid) and C17:0 (heptadecanoic acid), MUFA-C24:1 (nervonic acid), and PUFA-C22:5n-3 in *T. mediterraneus*, and SFA-C24:0 (lignoceric acid), total

Table 3. Mean and standard deviation (\pm SD) percentage (%) of fatty acids composition between males and females of *Chelon auratus*, *Trachurus mediterraneus*, and *Sardina pilchardus* collected from the five stations in the Gulf of Tunis, Tunisia.

Fatty acid	Mean of total fatty acids (mg/mL) \pm SD (%)					
	<i>C. auratus</i> ♂	<i>C. auratus</i> ♀	<i>T. mediterraneus</i> ♂	<i>T. mediterraneus</i> ♀	<i>S. pilchardus</i> ♂	<i>S. pilchardus</i> ♀
C12:0	0.13 \pm 0.02*	0.12 \pm 0.01	0.21 \pm 0.01 ^c	0.3 \pm 0.02	0.41 \pm 0.12*	0.42 \pm 0.14*
C14:0	5.49 \pm 0.22*	5.27 \pm 0.13	2.31 \pm 0.15*	2.27 \pm 0.21	2.63 \pm 0.04*	2.71 \pm 0.08*
C15:0	0.36 \pm 0.03*	0.38 \pm 0.02	0.49 \pm 0.03*	0.53 \pm 0.03	0.59 \pm 0.02*	0.63 \pm 0.03*
C16:0	22.10 \pm 3.15*	22.4 \pm 4.89	22.39 \pm 6.47*	22.43 \pm 7.22	23.72 \pm 5.42*	24.07 \pm 4.79*
C17:0	0.09 \pm 0.01*	0.07 \pm 0.01	0.63 \pm 0.02 ^a	0.59 \pm 0.01	0.31 \pm 0.01*	0.33 \pm 0.01*
C18:0	8.23 \pm 1.02*	8.18 \pm 1.24	8.19 \pm 0.14*	8.26 \pm 0.21	6.48 \pm 0.27*	6.39 \pm 0.07*
C20:0	0.19 \pm 0.03*	0.18 \pm 0.01	0.15 \pm 0.01*	0.16 \pm 0.01	0.22 \pm 0.02*	0.19 \pm 0.01*
C22:0	0.49 \pm 0.09*	0.42 \pm 0.02	0.31 \pm 0.02*	0.33 \pm 0.01	0.19 \pm 0.01*	0.2 \pm 0.02*
C24:0	1.08 \pm 0.03*	1.07 \pm 0.02	0.62 \pm 0.1*	0.58 \pm 0.13	0.23 \pm 0.01 ^a	0.19 \pm 0.02
Σ SFAs	38.16 \pm 2.31*	38.09 \pm 2.28	35.3 \pm 3.41*	35.45 \pm 3.27	34.78 \pm 7.22*	34.74 \pm 6.98
C16:1	2.04 \pm 0.03 ^a	2.1 \pm 0.02	2.29 \pm 0.18*	2.35 \pm 0.20	2.39 \pm 0.31*	2.34 \pm 0.30*
C17:1	0.19 \pm 0.01 ^b	0.22 \pm 0.01	0.28 \pm 0.02*	0.26 \pm 0.01	0.18 \pm 0.01*	0.15 \pm 0.03*
C18:1	14.25 \pm 0.5*	14.31 \pm 0.1	11.36 \pm 1.5*	11.28 \pm 1.12	18.51 \pm 1.22*	18.19 \pm 1.08*
C20:1	5.69 \pm 0.39*	5.67 \pm 0.27	0.66 \pm 0.12*	0.7 \pm 0.14	0.23 \pm 0.01*	0.24 \pm 0.01*
C22:1	0.26 \pm 0.42*	0.28 \pm 0.33	0.05 \pm 0.01*	0.04 \pm 0.01	0.56 \pm 0.01*	0.55 \pm 0.02*
C24:1	0.45 \pm 0.31*	0.51 \pm 0.03	0.82 \pm 0.02 ^c	0.91 \pm 0.01	0.66 \pm 0.03*	0.71 \pm 0.02*
Σ MUFAs	22.88 \pm 1.73*	23.09 \pm 1.23	15.46 \pm 1.45*	15.54 \pm 1.39	22.53 \pm 0.05^d	22.18 \pm 0.04
C18:2	2.49 \pm 0.01*	2.47 \pm 0.03	2.69 \pm 0.03*	2.65 \pm 0.02	1.73 \pm 0.01 ^c	1.81 \pm 0.02
C20:2	0.26 \pm 0.16*	0.30 \pm 0.01	0.31 \pm 0.06*	0.29 \pm 0.04	0.86 \pm 0.24*	0.86 \pm 0.24*
C18:3	1.92 \pm 0.04*	1.89 \pm 0.09	1.34 \pm 0.01*	1.38 \pm 0.03	1.37 \pm 0.05*	1.41 \pm 0.04*
C20:3n-3	0.06 \pm 0.01*	0.04 \pm 0.02	0.01 \pm 0.001*	0.02 \pm 0.02	0.28 \pm 0.01 ^c	0.32 \pm 0.01
C20:3n-6	0.13 \pm 0.01*	0.15 \pm 0.02	0.17 \pm 0.01*	0.15 \pm 0.01	0.43 \pm 0.01 ^c	0.51 \pm 0.02
C18:4n-3	0.14 \pm 0.02*	0.13 \pm 0.01	0.12 \pm 0.01*	0.11 \pm 0.01	0.36 \pm 0.14*	0.35 \pm 0.13*
C20:4n-6 (ARA)	4.97 \pm 0.01*	4.88 \pm 0.06	3.97 \pm 0.2*	3.88 \pm 0.3	5.02 \pm 0.3*	4.99 \pm 0.5*
C22:4n-6	0.14 \pm 0.01*	0.13 \pm 0.01	0.01 \pm 0.01*	0.02 \pm 0.01	0.04 \pm 0.01*	0.05 \pm 0.01*
C20:5n-3 (EPA)	7.18 \pm 0.13*	7.01 \pm 0.47	7.21 \pm 0.34*	7.33 \pm 0.26	6.22 \pm 1.03*	6.19 \pm 1.02*
C22:5n-3	0.73 \pm 0.01 ^b	0.78 \pm 0.02	1.32 \pm 0.01 ^a	1.29 \pm 0.01	0.69 \pm 0.04*	0.63 \pm 0.02*
C22:6n-3 (DHA)	30.79 \pm 3.22*	31.06 \pm 3.37	32.73 \pm 0.27*	33.01 \pm 0.27	27.73 \pm 6.32*	27.81 \pm 5.99
Σ PUFAs	48.81 \pm 3.33*	48.84 \pm 2.06	49.88 \pm 4.18*	50.13 \pm 5.01	44.73 \pm 6.08*	44.93 \pm 6.49
Σ PUFAs-n-3	39.03 \pm 1.14*	39.17 \pm 1.39	41.39 \pm 3.89*	41.47 \pm 4.06	34.92 \pm 5.22*	35.3 \pm 6.07
Σ PUFAs-n-6	5.21 \pm 0.46*	5.16 \pm 0.29	4.15 \pm 1.09*	4.05 \pm 0.98	5.49 \pm 0.1*	5.55 \pm 0.2

Abbreviation: ^{a-d}, significant differences between males and females at the $p < 0.05$, $p < 0.02$, $p < 0.01$, and $p < 0.001$, respectively; *, not significant; SFAs: saturated fatty acids; MUFAs: monounsaturated fatty acids; PUFAs: polyunsaturated fatty acids; EPA: eicosapentaenoic fatty acid; DHA: docosahexaenoic fatty acid; ARA: arachidonic fatty acid.

Table 4. Mean and standard deviation (\pm SD) percentage (%) of fatty acids composition between males and females of *Mullus barbatus*, *Gobius niger*, and *Trachinus draco* collected from the five stations in the Gulf of Tunis, Tunisia.

Fatty acid	Mean of total fatty acids (mg/mL) \pm SD (%)					
	<i>M. barbatus</i> ♂	<i>M. barbatus</i> ♀	<i>G. niger</i> ♂	<i>G. niger</i> ♀	<i>T. draco</i> ♂	<i>T. draco</i> ♀
C12:0	0.11 \pm 0.01 [*]	0.10 \pm 0.01	0.17 \pm 0.01 [*]	0.18 \pm 0.01	0.39 \pm 0.15 [*]	0.40 \pm 0.18
C14:0	3.27 \pm 0.01 ^a	3.31 \pm 0.02	2.68 \pm 0.02 ^b	2.51 \pm 0.03	3.81 \pm 0.02 [*]	3.73 \pm 0.03
C15:0	0.34 \pm 0.08 [*]	0.36 \pm 0.02	0.1 \pm 0.01 [*]	0.1 \pm 0.01	0.22 \pm 0.04 [*]	0.18 \pm 0.03
C16:0	28.73 \pm 3.46 [*]	28.51 \pm 3.13	29.63 \pm 5.27 [*]	25.42 \pm 4.12	30.99 \pm 2.42 ^a	26.19 \pm 1.67
C17:0	0.43 \pm 0.01 [*]	0.46 \pm 0.02	0.71 \pm 0.01 ^c	0.62 \pm 0.02	0.74 \pm 0.02 ^d	0.51 \pm 0.02
C18:0	7.12 \pm 0.33 [*]	7.09 \pm 0.01	6.29 \pm 0.01 ^d	4.32 \pm 0.02	7.25 \pm 1.03 ^e	3.49 \pm 0.05
C20:0	0.81 \pm 0.03 [*]	0.78 \pm 0.34	0.63 \pm 0.01 ^d	0.47 \pm 0.02	0.13 \pm 0.02 [*]	0.12 \pm 0.01
C22:0	0.35 \pm 0.03 [*]	0.34 \pm 0.01	0.12 \pm 0.01 ^c	0.05 \pm 0.01	0.14 \pm 0.01 ^a	0.11 \pm 0.01
C24:0	1.29 \pm 0.07 [*]	1.31 \pm 0.08	1.26 \pm 0.02 ^d	0.78 \pm 0.01	1.31 \pm 0.10 [*]	1.28 \pm 0.02
Σ SFAs	42.45 \pm 3.67[*]	42.26 \pm 4.01	41.59 \pm 4.16[*]	34.45 \pm 2.78	44.98 \pm 4.62^a	36.01 \pm 2.78
C16:1	4.43 \pm 0.14 [*]	4.39 \pm 0.10	4.31 \pm 0.03 ^d	2.18 \pm 0.01	4.16 \pm 0.2 [*]	4.27 \pm 0.02
C17:1	0.66 \pm 0.21 [*]	0.67 \pm 0.23	0.2 \pm 0.01 [*]	0.18 \pm 0.01	0.18 \pm 0.01 [*]	0.19 \pm 0.01
C18:1	6.59 \pm 0.23 [*]	6.72 \pm 0.19	4.22 \pm 0.03 ^d	5.72 \pm 0.01	5.12 \pm 0.41 [*]	5.31 \pm 0.27
C20:1	1.73 \pm 0.05 [*]	1.81 \pm 0.02	1.24 \pm 0.01 ^d	1.81 \pm 0.01	1.83 \pm 0.02 [*]	1.82 \pm 0.02
C22:1	0.21 \pm 0.02 [*]	0.22 \pm 0.01	0.16 \pm 0.01 [*]	0.18 \pm 0.03	0.25 \pm 0.06 [*]	0.27 \pm 0.04
C24:1	0.33 \pm 0.01 [*]	0.34 \pm 0.02	0.02 \pm 0.01 [*]	0.04 \pm 0.01	0.53 \pm 0.12 [*]	0.52 \pm 0.12
Σ MUFAs	13.95 \pm 1.17[*]	14.15 \pm 0.19	10.15 \pm 1.06[*]	10.11 \pm 1.12	12.07 \pm 1.84[*]	12.38 \pm 1.47
C18:2	2.48 \pm 0.35 [*]	2.56 \pm 0.36	1.36 \pm 0.01 ^d	1.58 \pm 0.03	3.27 \pm 0.57 [*]	3.59 \pm 0.61
C20:2	0.49 \pm 0.09 [*]	0.51 \pm 0.07	0.42 \pm 0.04 [*]	0.42 \pm 0.04	0.59 \pm 0.07 [*]	0.61 \pm 0.03
C18:3	3.31 \pm 0.01 [*]	3.29 \pm 0.02	2.16 \pm 0.13 ^a	2.39 \pm 0.03	2.61 \pm 0.01 ^d	3.22 \pm 0.01
C20:3n-3	2.66 \pm 0.27 [*]	2.60 \pm 0.25	1.87 \pm 0.01 ^d	2.59 \pm 0.11	2.01 \pm 0.02 ^d	2.18 \pm 0.01
C20:3n-6	0.64 \pm 0.01 [*]	0.65 \pm 0.07	0.12 \pm 0.01 [*]	0.2 \pm 0.14	0.12 \pm 0.04 [*]	0.14 \pm 0.04
C18:4n-3	0.33 \pm 0.17 [*]	0.34 \pm 0.15	0.1 \pm 0.01 [*]	0.1 \pm 0.01	0.31 \pm 0.13 [*]	0.30 \pm 0.13
C20:4n-6 (ARA)	1.78 \pm 0.09 [*]	1.81 \pm 0.02	3.21 \pm 0.13 [*]	3.21 \pm 0.13	2.64 \pm 0.02 ^d	3.05 \pm 0.02
C22:4n-6	0.02 \pm 0.01 [*]	0.03 \pm 0.01	0.01 \pm 0.001 [*]	0.01 \pm 0.001	0.02 \pm 0.01 [*]	0.03 \pm 0.01
C20:5n-3 (EPA)	6.82 \pm 0.2 [*]	6.87 \pm 0.34	5.66 \pm 0.15 ^c	9.22 \pm 1.13	3.12 \pm 0.03 ^d	9.05 \pm 0.02 ^d
C22:5n-3	1.29 \pm 0.01 [*]	1.27 \pm 0.01	0.12 \pm 0.01 ^b	0.16 \pm 0.01	0.77 \pm 0.41 [*]	0.94 \pm 0.41
C22:6n-3 (DHA)	12.78 \pm 2.44 [*]	12.81 \pm 0.253	13.27 \pm 2.13 [*]	16.5 \pm 2.27	10.42 \pm 1.27 [*]	13.59 \pm 1.72
Σ PUFAs	32.6 \pm 3.26[*]	32.74 \pm 3.54	28.3 \pm 1.25^b	36.38 \pm 3.14	25.88 \pm 3.09^b	36.7 \pm 3.31
Σ PUFAs-n-3	23.88 \pm 3.14[*]	23.89 \pm 3.65	21.02 \pm 1.09^c	28.57 \pm 2.05	16.63 \pm 1.14^c	26.06 \pm 2.07
Σ PUFAs-n-6	2.44 \pm 0.02[*]	2.43 \pm 0.01	3.34 \pm 0.01[*]	3.43 \pm 0.12	2.78 \pm 0.02^d	3.22 \pm 0.03

Abbreviation: ^{a-d}, significant differences between males and females at the $p < 0.05$, $p < 0.02$, $p < 0.01$, and $p < 0.001$, respectively; ^{*}, not significant; SFAs: saturated fatty acids; MUFAs: monounsaturated fatty acids; PUFAs: polyunsaturated fatty acids; EPA: eicosapentaenoic fatty acid; DHA: docosahexaenoic fatty acid; ARA: arachidonic fatty acid.

MUFAs, and PUFA-C18:2 (linoleic acid, LA), C20:3n-3 (docosatrienoic acid) and 3n-6 (Dihomo- γ -linolenic acid, DGLA) in *S. pilchardus* (Table 3). In *M. barbatus*, a significant difference was only shown in SFA-C14:0 (myristic acid) between males and females (Table 4). However, in *G. niger*, significant differences were recorded

in SFA-C14:0, C17:0, and C22:0 (docosanoic acid), C18:0 (stearic acid), C20:0 (eicosanoic acid), and C24:0, MUFA-C16:1, C18:1 (oleic acid), and C20:1 (gondoic acid), and total PUFAs dominated by C18:2, C18:3 (linolenic acid), C20:3n-3, C20:5n-3 (EPA), C22:5n-3, and total PUFAs-n-3 and -n-6 family. But, in *T. draco*,

significant differences were observed in total SFAs represented by C16:0 and C22:0, C17:0, and C18:0, total PUFAs prevailed by C18:3, C20:3n-3, C20:4n-6 (ARA), and C20:5n-3 (EPA), and total PUFAs-n-3 and -n-6 family (Table 3). In addition, as indicated in Figure 3b, the PCA of fatty acid composition percentages between and within males and females of the six species explained a total variance of 90.1% and showed that the first component (PC1) accounted for 72.1% of the total variation between fatty acid composition. Besides, the PC1 was characterized by high positive correlations (loads) of males and females of both *S. pilchardus* and *C. auratus* with total MUFA and PUFA-n-6, C20:4n-6, and C22:6n-3, and males and females of *T. mediterraneus* with total PUFA, PUFA-n-3, C20:5n3, and a strong negative loading of males and females of *M. barbatus*, *G. niger*, and *T. draco* with total SFA. However, the second component (PC2) accounted for only 18% of the total variance and created a strong positive loading of males of both *G. niger* and *T. draco* with total SFA, as well as loading of males and females of *S. pilchardus* and *C. auratus* with total MUFA, PUFA-n-6, C20:4n-6, and C22:6n-3. But, its negative correlation was characterized by the loading of males and females of both *M. barbatus* and *T. mediterraneus* and females of both *G. niger* and *T. draco* with total PUFA, PUFA-n-3, C20:5n3. Moreover, the PC1 axis differentiated and separated males and females of *S. pilchardus*, *C. auratus*, and *T. mediterraneus* in the positive part and those of *M. barbatus*, *G. niger*, and *T. draco* in the negative part. Nevertheless, the PC2 axis segregated both sexes of *S. pilchardus* and *C. auratus* and only males of *G. niger* and *T. draco* in the positive part, and those of *M. barbatus* and *T. mediterraneus* in the negative part together with females of *G. niger* and *T. draco*.

3.3. Otolith shape variation

Levene's and Wilk's λ tests confirmed that all values of otolith shape variance were equally and normally distributed ($p > 0.05$). At the interspecific level, Wilk's λ test

values showed a statistically significant shape difference ($p < 0.0001$) in the left and right otoliths' shapes, i.e. there was a bilateral asymmetry (Table 5). Similarly, Fisher's distance (D) also showed a significant shape difference ($p < 0.05$), i.e. bilateral asymmetry, in the left and right otoliths only between males and females of *C. auratus* ($D = 2.087$), *G. niger* ($D = 1.812$), and *T. mediterraneus* ($D = 1.726$) (Table 7). As shown in Figure 4a, the barycenter projection based on EFDs of the contour shape of the left and right otoliths from individuals of the six species on the first axes F1 and F2 of the DFA revealed that the two axes explained 47.91% and 21.28% of the total variation, respectively. Therefore, the otoliths' shapes of the six species were segregated on the positive and negative parts of the F1 and F2 axes. The two axes accounted for 69.19% of the total shape variance and showed the presence of two distinct main clusters or groups of otoliths. The first group segregated on the positive part of the F1 axis and comprised the otoliths of *M. barbatus*, *G. niger*, and *T. draco*, while the second group included *T. mediterraneus*, *S. pilchardus*, and *C. auratus* in the negative part. However, the F2 axis separated the otoliths of *S. pilchardus*, *T. mediterraneus*, *M. barbatus*, and *G. niger* in the positive part and those of *C. auratus* and *T. draco* in the negative.

At the intraspecific level, Wilk's λ test revealed a significant intersexual shape difference ($p < 0.05$), i.e. there was a bilateral asymmetry, in the left and right otoliths' shapes only in *G. niger* ($p = 0.016$) and *T. draco* ($p = 0.045$). On the contrary, a significant shape similarity, i.e. symmetry, was found in *C. auratus* ($p = 0.172$), *T. mediterraneus* ($p = 0.374$), *S. pilchardus* ($p = 0.901$), and *M. barbatus* ($p = 0.297$) (Table 6). In addition, Fisher's distance (D) matrix of the left and right otolith shape values within males and females within each species revealed significant shape bilateral asymmetry ($p < 0.05$) only among females of *G. niger* ($D = 1.520$) and among males of *T. draco* ($D = 1.825$) (Table 7). Moreover, as shown in Figure 4b, the barycenter projection based on EFDs of the contour shape of the left

Table 5. Wilk's lambda (λ) test of the left and right otoliths shape variance distance approximation values between individuals of the six species collected from the five stations in the Gulf of Tunis, Tunisia.

Parameter	Value
Lambda (λ)	0.0000
F (Observed value)	5780.2006
F (Critical value)	1.1292
DF1	385
DF2	3440
p-value	< 0.0001
Alpha	0.05

The value marked in bold is statistically significant ($p < 0.0001$).

Table 6. Wilk's lambda (λ) test of the left and right otoliths' shape variance distance approximation values between males and females within each of the six species collected from the five stations in the Gulf of Tunis, Tunisia.

Species	Lambda (λ)	F (Observed value)	F (Critical value)	DF1	DF2	p-value
<i>C. auratus</i>	0.0297	1.1667	1.3076	231	121	0.1722
<i>T. mediterraneus</i>	0.0585	1.0501	1.2790	231	154	0.3738
<i>S. pilchardus</i>	0.5035	0.7301	1.5170	77	57	0.9011
<i>G. niger</i>	0.0667	1.3393	1.2494	231	211	0.0156
<i>T. draco</i>	0.0144	1.3462	1.3345	231	100	0.0451
<i>M. barbatus</i>	0.0341	1.0917	1.3076	231	121	0.2971

The values marked in bold are statistically significant ($p < 0.05$).

Table 7. Fisher's distance (D) mean values of the left and right otoliths among and within males (σ) and females (ρ) and the two sexes combined (σ and ρ) of the six species collected from the five stations in the Gulf of Tunis, Tunisia.

Species	Males (σ)	Females (ρ)	Fisher's distance (σ and ρ)	p-value (σ and ρ)
<i>C. auratus</i>	1.2490	2.0870	2.0870	0.0053
<i>T. mediterraneus</i>	0.9150	1.4065	1.7255	0.0183
<i>S. pilchardus</i>	0.8767	0.5938	0.7301	0.9011
<i>M. barbatus</i>	1.0485	0.7874	0.8746	0.6981
<i>G. niger</i>	1.1882	1.5203	1.8123	0.0058
<i>T. draco</i>	1.8253	1.0102	1.5579	0.0738

The values marked in bold are statistically significant ($p < 0.05$).

and right otoliths between and within males and females of the six species on the first axes F1 and F2 of the DFA revealed that the two axes explained 98.91% and 0.89% of the total variation, respectively. Therefore, the left and right otolith shapes of either males or females or both of the six species were separated in the positive and negative parts of the F1 axis. The two axes accounted for 99.80% of the total shape variance and showed the left and right otoliths from both males and females of *S. pilchardus*, *C. auratus*, and *T. mediterraneus* in the positive part of F1. However, the F1 axis showed the separation and segregation of the left and right otoliths of males and females of *M. barbatus*, *G. niger*, and *T. draco* in the negative part. The F2 axis segregated the left and right otoliths of both males and females of *S. pilchardus* and *C. auratus*, males of *G. niger* in the middle, and males of *M. barbatus* and *T. draco* in the positive part. While the left and right otoliths of both males and females of *T. mediterraneus* and those of females of *M. barbatus*, *G. niger*, and *T. draco* were segregated in the negative part.

Similarly, as appeared in Figure 5, the HAC of the six species based on the variance in the otolith shape values revealed a clear distinction between the six species, with

two primary groups or clusters formed. In the first clade, both *M. barbatus* and *G. niger* were grouped into one main clade and joined to that of *T. draco*, while the second clade included both *T. mediterraneus* and *S. pilchardus* in a single clade nested within the *C. auratus* clade.

3.4. Consistency between variations in fatty acid composition and otolith shape

As indicated in Figure 6, the barycenter projection based on PCA using EFDs of the contour shape of the left and right otoliths and percentages of fatty acid composition between males and females of the six species revealed that the six species were discriminated from each other by the PC1 and PC2 axes, with a total variance value equal to 87.4% between the two variables. Of these two axes, the PC1 axis accounted for 64.1% of the total variance and segregated high negative loading of left and right otolith shape asymmetry observed in *G. niger* and *T. draco* and symmetry in *M. barbatus* with total SFAs and strong positive loading of total PUFAs and MUFAs, and PUFA-C20:5n-3, C20:4n-6, C22:6n-3, n-3, and n-6 with left and right otolith shape symmetry detected in *C. auratus*, *T. mediterraneus*, and *S. pilchardus*. In addition, the PC2

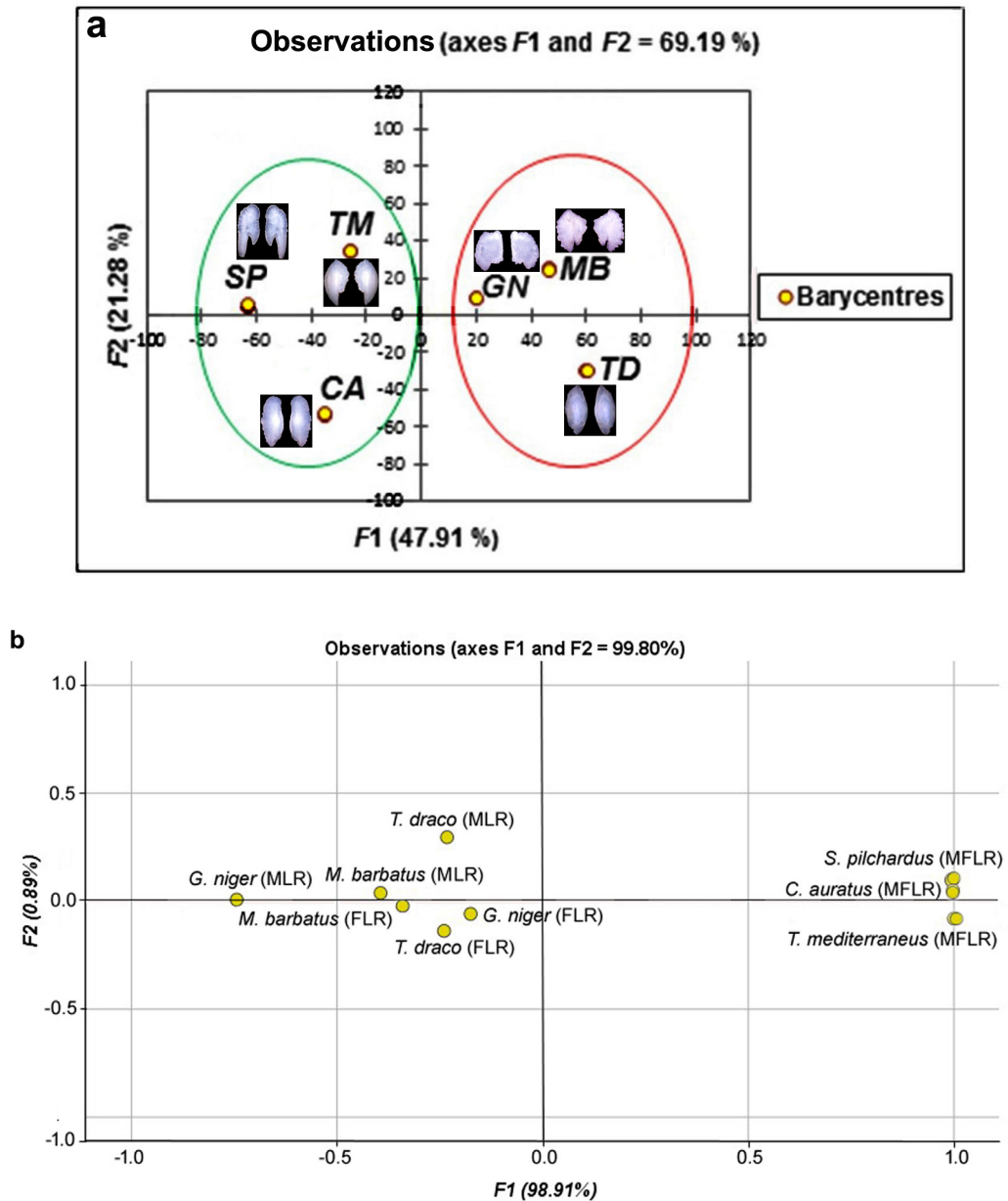


Figure 4. Principal component analysis (PCA) graph (biplot) showing the barycenter (●) projection of the left (L) and right (R) otolith shape values between (a) and within (b) males (M) and females (F) of the six species collected from the five stations in the Gulf of Tunis, Tunisia. TM: *T. mediterraneus*; SP: *S. pilchardus*; CA: *C. auratus*; MB: *M. barbatus*; GN: *G. niger*; TD: *T. draco*.

axis accounted for 23.3% of the total variance and showed a strong positive loading of otolith shape asymmetry recorded in males of *G. niger* and *T. draco* and symmetry among males and females of *S. pilchardus* and females of *C. auratus* with total MUFAs and PUFA-C22:6n-3, C20:4n-6, and n-6. However, the otolith shape symmetry detected among males and females of *M. barbatus* and *T. mediterraneus*, and asymmetry in females of *G. niger* and

T. draco segregated in the negative part, together with symmetry in males of *C. auratus*, was loaded with total PUFAs, C20:5n-3, and PUFA-n-3.

4. Discussion

Recent studies have shown that lipids are the principal structural and energetic components of marine organisms, and therefore, their content may vary between species

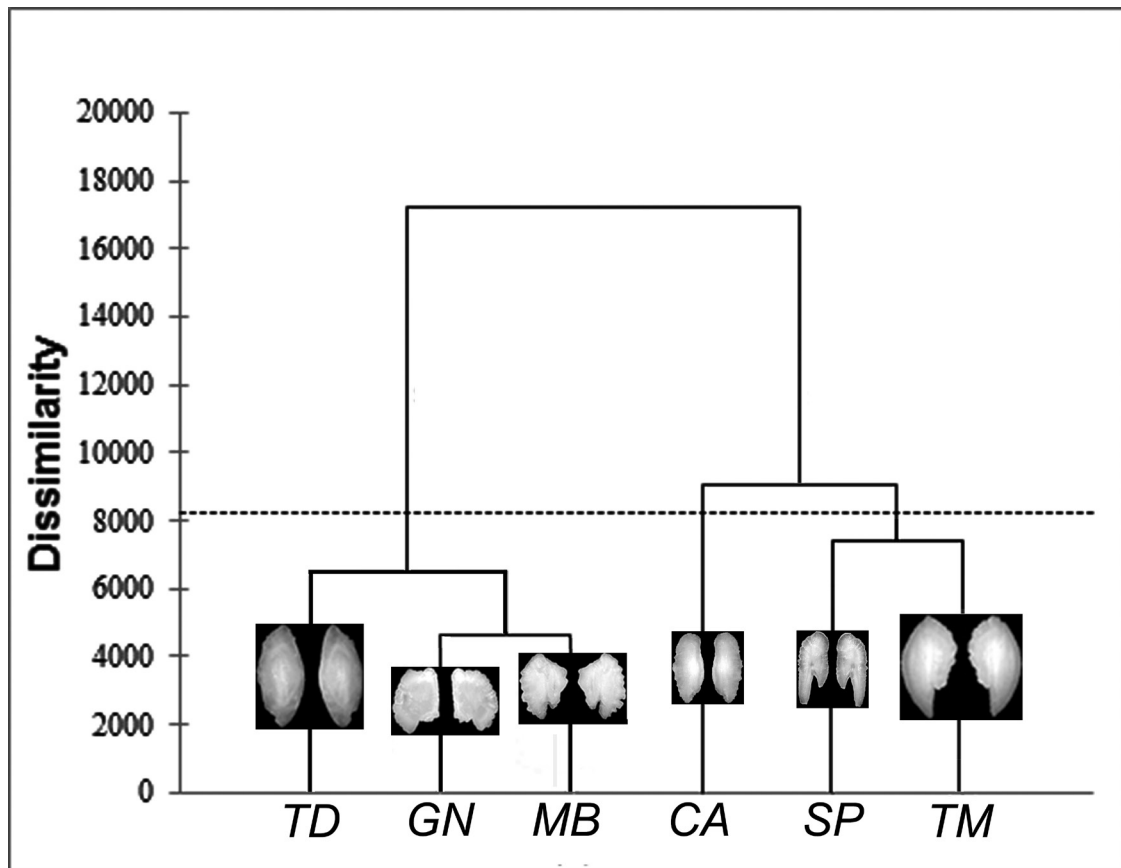


Figure 5. Hierarchical ascending classification (HAC) dendrogram generated based on the left and right otoliths shape values of dissimilarity between individuals of the six species collected from the five stations in the Gulf of Tunis, Tunisia. TM: *T. mediterraneus*; SP: *S. pilchardus*; CA: *C. auratus*; MB: *M. barbatus*; GN: *G. niger*; TD: *T. draco*.

according to their physiological state and locomotion (Voronin et al., 2021). In addition, fatty acids, which are fractional components of lipids, are highly polyfunctional and directly depend not only on the physiological state but also on environmental factors, such as temperature and hydrostatic pressure (Nemova et al., 2014). At the interspecific level, the fatty acid composition was shown to be closely related to the strata depth and diet content of the fish species examined here. For example, *T. mediterraneus*, *S. pilchardus*, and *C. auratus*, which are benthopelagic to pelagic species and feed on a wide variety of small organisms, including crustaceans, insects, and plankton, had significantly higher content ($p < 0.05$) of PUFAs, especially DHA, than *M. barbatus*, *G. niger*, and *T. draco*, which are benthic species, live near the sea bottom and are restricted in their feeding on benthic organisms (Shulman and Jakovleva, 1983). In addition, based on PCA using the two-dimensional model, the results showed that *M. barbatus*, *G. niger*, and *T. draco* had a strong correlation with SFAs palmitic acid (C16:0) and stearic acid (C18:0),

while the *T. mediterraneus*, *S. pilchardus*, and *C. auratus* had the highest contents of MUFAs and PUFAs, and their major compounds, including PUFA-n-3, n-6, C20:5n-3, C22:6n-3, and C20:5n-3. As described by Voronin et al. (2021), this difference in the content of PUFAs may be related not only to the different spectra of food available at different depths but also to the higher locomotor activity characteristics of these species. Besides, Voronin et al. (2021) confirmed that the DHA content in muscle tissues of redfish *Sebastes mentella* increased with depth, as the increase in membrane microviscosity and flexibility is regulated by PUFAs. Moreover, here we found that PUFA-3 and -6 content was also higher in *T. mediterraneus*, *S. pilchardus*, and *C. auratus* than in *M. barbatus*, *G. niger*, and *T. draco*, and this can be attributed to the effect of temperature, depth, or hydrostatic pressure as well as the fish's natural mobility under certain habitat conditions, such as turbulent flows and currents (Shulman and Yuneva, 1990). Therefore, we can suggest here that the obvious differences in the content of PUFA, particularly

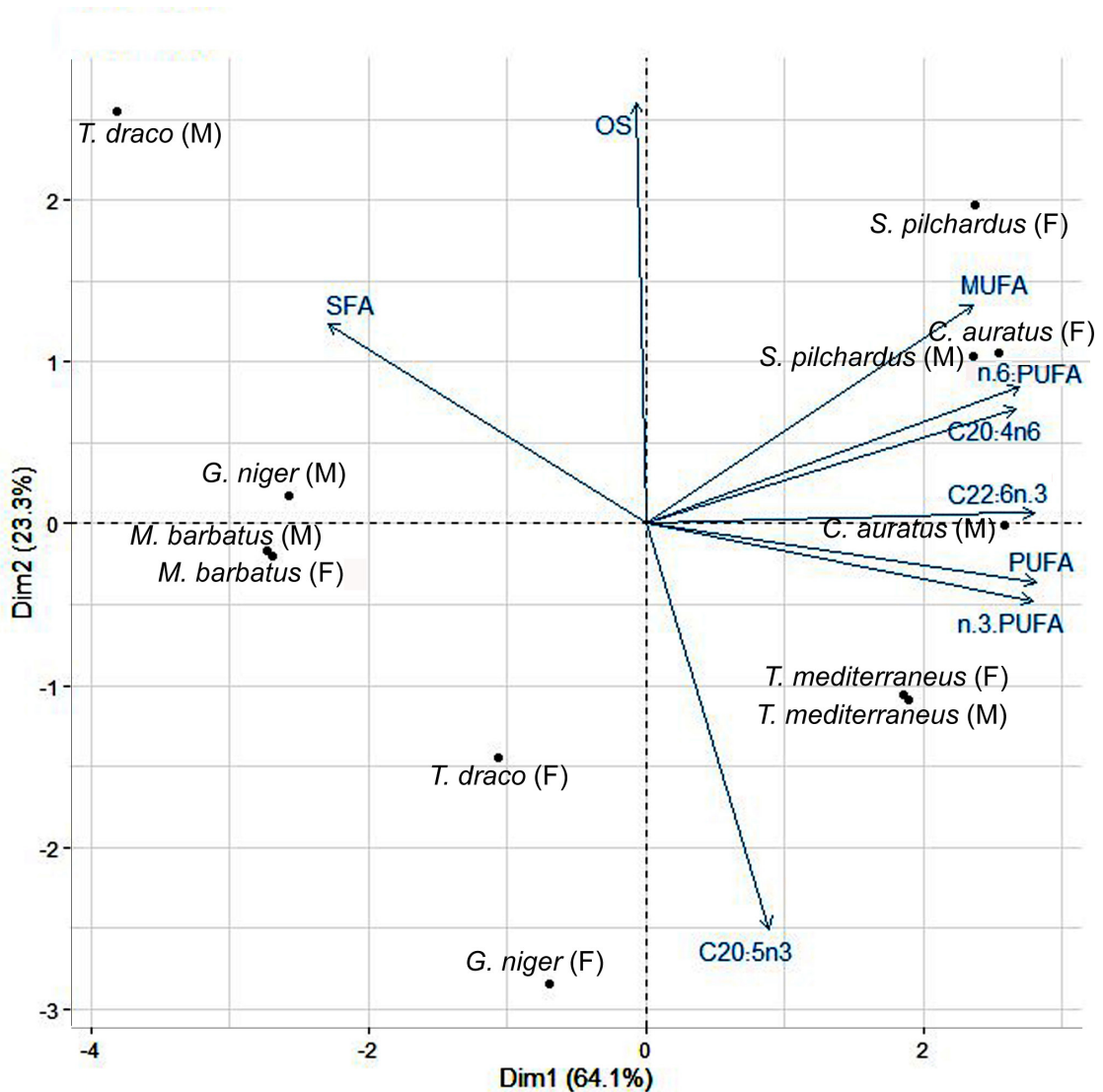


Figure 6. Principal component analysis (PCA) graph (biplot) showing the consistency between the variation in the otoliths shape (OS) and the variation in fatty acid composition between and within males (M) and females (F) of the six species collected from the five stations in the Gulf of Tunis, Tunisia.

EPA and -3 and -6, MUFA-C18:1, and SFA-C16:0 and C18:0 between *T. mediterraneus*, *S. pilchardus*, and *C. auratus*, which are benthopelagic to pelagic species, and *M. barbatus*, *G. niger*, and *T. draco*, which assume mostly benthic life, could be due to the difference in metabolism, environmental factors (e.g., temperature and hydrostatic pressure), depth strata and diet content, and locomotor activity of these species.

On the other hand, otolith shape is a genetically controlled trait that has so far been used as a key for species identification (Assis, 2005; Yedier and Bostanci, 2022; Mejri et al., 2022a). This phenotype trait was controlled not only by the genotype of individuals but also by the interaction of the latter with the environment; therefore,

the shape of otoliths has been suggested to recognize the living environments inhabited by a species or population and to reconstruct their life history (Vignon and Morat, 2010). In this regard, several studies have shown that the biotic and abiotic environmental conditions where the fish live are among the most prominent factors, which influence the otolith morphological variability (Vignon and Morat, 2010; Ben Labidi et al., 2020a, 2020b; Khedher et al., 2021; Çöl and Yilmaz, 2022; Mejri et al., 2022a, 2022b; Ben Mohamed et al., 2023) and lead to developmental abnormalities and aberrations observed in many species (Carvalho et al., 2019; Yedier and Bostanci, 2019, 2020; De Carvalho Lapuch et al., 2022; Yedier, 2022; Yedier et al., 2023). In the present study, the shape of otoliths showed

a clear variation, i.e. bilateral asymmetry, on the left and right sides between the six species examined, which inhabit different trophic niches at different latitudes and longitudes. This finding is consistent with that found by Lombarte et al. (2010) who explained the difference in otolith shape between benthic and pelagic species in light of their ecomorphological adaptation to biotic (e.g., food) and abiotic (e.g., temperature) factors in their niches that may even mask ontogenic influences on shape. In addition, the contour shape asymmetry results are in agreement with those published on the sparid *Diplodus annularis* (Trojette et al., 2015), *Pagellus erythrinus* (Mejri et al., 2022b), *Boops boops* (Ben Labidi et al., 2020a, 2020b) and *D. vulgaris* (Khedher et al., 2021), which inhabit different habitats in Tunisian waters, including the Gulf of Tunis. Moreover, Ramcharitar et al. (2004) found a close correlation between the shape of the saccular otoliths and the hearing capabilities of the inner ear by the presence of deeply grooved sulci, two-planar saccular sensory epithelia, and a unique orientation pattern of ciliary bundles of sensory hair cells on the saccular sensory epithelium. Furthermore, Lychakov and Rebane (1993) indicated that the directional model of otoliths revealed shape-dependent anisotropy, suggesting that the otoliths' shape is the origin of orientation recognition and balance maintenance. Recently, Yedier and Bostanci (2022) reported that variations in the cytochrome c oxidase subunit I (COI) gene are consistent with variations in the otolith shape and confirmed that otoliths possess phylogenetic signals to differentiate between the *Scorpaena* species. Among these six species examined here in Tunisian waters, Khemiri et al. (2014) used otolith chemistry analysis to determine the stock structure of *S. pilchardus* and *Engraulis encrasicolus* in the open sea and coastal area of the Gulf of Gabes and found a clear distinction between the two species, as well as a clear discreteness of the open sea and inshore small pelagic groups. Fatnassi et al. (2017) found asymmetry in the shape of the left and right otoliths only among *T. draco* females collected from the Bizerte station (northern Tunisia), and sexual dimorphism has been found only in the width and area of the otoliths. Bouriga et al. (2021) reported that the mean value of otolith mass asymmetry (X) varied from -0.2 to 0.2 , and only the pelagic *C. auratus*, *T. mediterraneus*, and *S. pilchardus* showed values that exceeded the critical limits, especially *T. mediterraneus* ($-0.3665 < X < 0.3379$). Also, they attributed this variation in X within the latter species to its physiological state, habitat, and biotic and abiotic environmental factors. As previously reported, the Gulf of Tunis suffers from several pollutants, such as metal pollutants, industrial and urban discharges, and organic and mineral inputs (El Kateb et al., 2018). In addition, El Kateb et al. (2018) mentioned that the pH in the Gulf varies from 7.8 and 8.0, the dissolved

oxygen (DO) values at the seafloor differ from 7.1 to 7.8 mg/L at most stations, the bottom water temperatures fluctuate around 27.3 °C, the values of the hydrogen (HI) and oxygen (OI) indices vary from 143 to 378 mg HC/g, and the total organic carbon (TOC) ranges from 128 to 1083 mg CO₂/g. Moreover, Ben Ltaief et al. (2015) reported that the salinity in the Gulf is high (ranging from 37.5 to 39.25 psu). Therefore, the pollution state and high temperature, salinity, pH, and CO₂ can lead to eutrophication and acidification of the water, and as a result, can affect the shape and size of the otoliths. The effect of acidification on the development of otolith shape and size has also been documented by Munday et al. (2011), particularly at pH 7.6 and 1721 μatm CO₂. Accordingly, we can suggest that the physiological, biotic (food quality and quantity), abiotic (temperature and salinity), and pollution factors are probably among the main reasons for the difference in the shape of otoliths between these six species.

At the intraspecific level, analysis of fatty acid composition between males and females within the six species showed that both *G. niger* and *T. draco*, which are benthic species and feed on a wide variety of invertebrates, displayed a high differential correlation with the majority of SFAs, MUFAs, and PUFAs, compared to other species. Of these fatty acids, SFA- C17:0, C18:0, and C22:0 and PUFA-C18:3, C20:3n-3, C20:5n-3 (EPA), and PUFAs-n-3 were predominated and shared in the two species. As far as known, eicosapentaenoic acid (EPA, C20:5n-3) functionally plays vital roles in the reproduction, immunity efficiency, osmoregulation (Bret and Müller-Navarra, 1997), growth, development, and maintenance of brain structure and function (Horrocks and Akhlaq, 2004) in animals. In addition, PUFA-n-3 has a potential effect on the development of the audiovestibular system of fish, especially the biomineralization of otolith, which forms an organic fraction of 0.2% to 10% of the total material (Degens et al., 1969). Therefore, we can conclude that the significant increase of these aforementioned fatty acids in these benthic species may be correlated with the growth, development, and reproduction period, which starts in March and lasts during October in *G. niger* (Filiz and Toğulga, 2009) and September in *T. draco* (Ak and Genç, 2013), and development and biomineralization of their otoliths, which also exhibited significant intersexual shape differences, compared to other species.

In addition, we found that the shape of left and right otoliths differed between males and females within the six species regardless of the depth of their living environment. For example, the asymmetry of otolith shape on the left and right sides was found to differ significantly ($p < 0.05$) only between males and females of *G. niger* and *T. draco* living at different depths of 30 to 80 m (Kara and Quignard, 2019) and 15 to 150 m (Roux, 1990), respectively. Similar

intersexual results have been found by Ben Mohamed et al. (2023) in *M. barbatus*, Mejri et al. (2022a) in *Liza aurata* and *C. ramada*, Khedher et al. (2017) in *Mugil cephalus*, and Espino-Barr et al. (2013) in *M. curema*. Some other researchers have also shown that significant asymmetry in otolith shape is an indicator of developmental instability caused by biotic (e.g., parasitism) or abiotic (e.g., dietary input) stress (Mille, 2015). Given all these factors discussed above, these may be potential factors to explain the asymmetry that was only found in these three current species.

Regarding the relationship between the shape of otoliths and the differentiation of these six species, it was found that the shape of otoliths clearly classified these species into two main clades consistent with the nature of their living habits in the water column and the type of food they eat. The first clade clustered *M. barbatus*, *G. niger*, and *T. draco* that assumes mostly a benthic life and feeds on small invertebrates and fish (Roux, 1990; Özbilgin et al., 2004; Kara and Quignard, 2019), while the second grouped *S. pilchardus*, *T. mediterraneus*, and *C. auratus* that are benthopelagic to pelagic species and feed on small organisms, including crustaceans, insects, and plankton (Ben-Tuvia, 1986; Thomson, 1990; van der Lingen et al., 2009; Georgieva et al., 2019). This result is consistent with that of Bouriga et al. (2021) who assigned these six species into two groups, pelagic and benthic fishes, based on the variation in otolith mass asymmetry (X). Likewise, Lombarte et al. (2010) indicated a clear correspondence between relative size, otolith shape, and nutritional status, with most benthic feeders having the largest sagittae relative to body size, and pelagic ones with small, rounded sagittae.

As regards the consistency between the variation in the fatty acid composition and the variation in the shape of otoliths among the six examined species, it was shown that the otolith shape asymmetry found in *G. niger* and *T. draco* and symmetry in *M. barbatus* was loaded with the higher content of SFAs, especially C16:0. However, the shape symmetry detected in *S. pilchardus*, *C. auratus*, and *T. mediterraneus* was loaded with the highest levels of PUFAs (EPA, DHA, ARA, and -3 and -6) and MUFAs (C18:1). Accordingly, we can conclude that the SFAs, MUFAs, PUFAs, and their major compounds were linked with the growth and asymmetry of otoliths in these species. This is likely consistent with the findings by Sargent et al. (1999) who reported that highly PUFAs, especially n-3, are an essential source of energy for fish that they cannot synthesize and among which EPA, DHA, and n-3 are involved in the growth, development, and survival of marine fish. In addition, Amara et al. (2007) showed that the growth of otolith in larvae and juveniles is related to an individual condition index, estimated from fish lipid composition, which in turn depends on zooplankton

biomass (Suthers, 1996). However, Mahé et al. (2019) identified that the concentration of PUFAs in fish diet did not have a significant effect on otolith shape, adding that the results do not rule out the potential influence of dietary PUFA-n-3 content on otolith morphogenesis below the minimum threshold. Therefore, it is worth assuming that the obvious asymmetry in otolith shape and the highest content of PUFAs (particularly EPA) detected in *C. auratus* and *T. mediterraneus* are consistent with the feeding habits and benthopelagic nature of these species, which require more energy and develop the audiovestibular system necessary for higher locomotor activity and hearing for these species. However, the deviation of both *S. pilchardus*, which showed significant otolith symmetry and high PUFAs content, and *G. niger*, which displayed otolith asymmetry and low PUFAs content, from this assumption can be interpreted as follows: *S. pilchardus* is pelagic to benthopelagic, i.e. transitional species, highly opportunistic and flexible microphagous foragers, living at depths of 10 to 100 m (Tous et al., 2015), and searching for local planktonic crustaceans (van der Lingen et al., 2009). Therefore, it may need more energy and development of the audiovestibular system necessary for higher locomotor activity and hearing characteristics. In contrast, *G. niger* is an omnivorous benthic species, inhabiting coastal marine waters up to 80 m deep, but mostly between the surface and 30 m, and feeding on a variety of invertebrates (Kara and Quignard, 2019). Consequently, it may not require more energy and development of the audiovestibular system necessary for the lower locomotor activity and hearing characteristics displayed by transitional benthopelagic species.

5. Conclusion

At the interspecific level, Tukey's test with one-way ANOVA indicated significant differences in the total percentages of saturated (SFAs), polyunsaturated (PUFAs), and monounsaturated (MUFAs) fatty acids between individuals of the six species, and only between males and females of *Gobius niger*, and *Trachinus draco*. In addition, Wilk's λ test showed a statistically significant difference (asymmetry) in the shape of left and right otoliths between the six species. Moreover, discriminant function analysis (DFA) based on both fatty acid composition and otolith shape separated the six species into two main distinct clusters or groups. The first group comprised *M. barbatus*, *G. niger*, and *T. draco*, which assume a benthic life, while the second included *S. pilchardus*, *T. mediterraneus*, and *C. auratus*, which are benthopelagic to pelagic species. At the intraspecific level, principal component analysis (PCA) based on variation in fatty acid composition clearly differentiated and separated males and females of the six species either in the positive or negative parts of the first PC1 and PC2

axes, with the sexes of *G. niger* and *T. draco* segregated in both parts. Besides, Wilk's λ test revealed a statistically significant difference (asymmetry) in the shape of left and right otoliths between males and females of *C. auratus*, *T. mediterraneus*, and *G. niger*. However, Fisher's distance matrix indicated a significant asymmetry only between males and females of *G. niger* and *T. draco*. Both DFA and hierarchical ascending classification (HAC), based on the differences in the otolith shape values, separated the six species into two groups congruent to those obtained from the fatty acid composition analysis. Moreover, combined analyses of the variation in both fatty acid composition and shape of the otoliths among and within males and females of the six showed that the otolith shape asymmetry found in *G. niger* and *T. draco* and symmetry in *M. barbatus* was loaded with the higher content of SFAs, especially C16:0. However, the shape symmetry detected in *S. pilchardus*, *C. auratus*, and *T. mediterraneus* was loaded with the highest levels of PUFAs (EPA, DHA, ARA, and -3 and -6) and MUFAs (C18:1). This observed variation in both fatty acid composition and otolith shape within and between the six species was explained in the light of the ecomorphological adaptation of these species to physiological state, biotic and abiotic environmental factors, including temperature and hydrostatic pressure, depth strata, feeding habits, and locomotor activity for these species. These results indicated that variability in the fatty acid composition is consistent with variation in the otolith shape, and both have combined characteristic signals for these species and validated the use of fatty acid composition and otolith shape analyses as an effective approach to discriminate between and within these species.

References

- Ak O, Genç Y (2013). Growth and reproduction of the greater weever (*Trachinus draco* L., 1758) along the eastern coast of the Black Sea. *Journal of Black Sea/Mediterranean Environment* 19 (1): 95-110.
- Amara R, Meziane T, Gilliers C, Hermel G, Laffargue P (2007). Growth and condition indices in juvenile sole *Solea solea* measured to assess the quality of essential fish habitat. *Marine Ecology Progress Series* 351: 201-208. <https://doi.org/10.3354/meps07154>
- Assis CA (2005). The utricular otoliths, lapilli, of teleosts: their morphology and relevance for species identification and systematics studies. *Scientia Marina* 69 (2): 259-273. <https://doi.org/10.3989/SCIMAR.2005.69N2259>
- Bakkari W, Mejri M, Ben Mohamed S, Chalh A, Quignard J-P et al. (2020). Shape and symmetry in the otolith of two different species *Mullus barbatus* and *Mullus surmuletus* (Actinopterygii: Perciformes: Mullidae) in Tunisian waters. *Acta Ichthyologica et Piscatoria* 50 (2): 151-159. <https://doi.org/10.3750/AIEP/02760>
- Bang A, Grønkvær P (2005). Otolith size-at-hatch reveals embryonic oxygen consumption in the zebrafish, *Danio rerio*. *Marine Biology* 147: 1419-1423. <https://doi.org/10.1007/S00227-005-0037-Y>
- Béarez P, Schwarzhans W (2013). *Robaloscion*, a new genus for *Sciaena wieneri* Sauvage, 1883 (Teleostei, Sciaenidae) from the southeastern Pacific, with clarification of the taxonomic status of *Sciaena starksi* Evermann and Radcliffe, 1917. *Cybium* 37 (4): 273-279. <https://doi.org/10.26028/cybium/2013-374-006>
- Begg GA, Brown RW (2000). Stock identification of haddock *Melanogrammus aeglefinus* on Georges Bank based on otolith shape analysis. *Transactions of the American Fisheries Society* 129: 935-945. [https://doi.org/10.1577/1548-8659\(2000\)129<0935:SIOHMA>2.3.CO;2](https://doi.org/10.1577/1548-8659(2000)129<0935:SIOHMA>2.3.CO;2)
- Ben Labidi M, Mejri M, Shahin AA., Quignard JP, Trabelsi M et al. (2020a). Stock discrimination of the bogues Boops boops (Actinopterygii, Sparidae) from two Tunisian marine lagoons using the otolith shape. *Acta Ichthyologica et Piscatoria* 50: 413-422. <https://doi.org/10.3750/AIEP/02978>

Acknowledgments

The authors are grateful to all the people and fishermen who helped us collect the individuals of the six species from the five stations in the Gulf of Tunis.

Contribution of authors

NB, WRB, SB, and ABF conceptualized, designed, supervised, and wrote the main draft. MFAH carried out the experimental work, collected the samples, and analyzed the data. AABS wrote, revised, and edited the final manuscript. J-P Q and MT read and validated the manuscript. All authors read and approved the final version of the manuscript.

Ethics approval

The Laboratory of Ecology, Biology and Physiology of Aquatic Organisms and Laboratory of Biodiversity, Biotechnology and Climate Change, Faculty of Sciences of Tunis, University of Tunis El Manar, Tunis, Tunisia, has approved this research. In addition, all procedures in this study were performed following the guidelines for the Proper Conduct of Animal Experiments outlined by the University of Tunis El Manar, Tunis, Tunisia (No. 1474 certificated on August 14th, 1995), as well as all applicable international, national, and/or institutional guidelines for the care and use of animals in Research.

Conflicts of interest

The authors declare that they have no known competing financial interests or personal relationships that could have appeared to influence the work presented in the paper.

- Ben Labidi M, Mejri M, Shahin AAB, Quignard JP, Trabelsi M et al. (2020b). Otolith fluctuating asymmetry in Boops boops (Actinopterygii, Sparidae) from two marine lagoons (Bizerte and Kelibia) in Tunisian waters. *Journal of the Marine Biological Association of the United Kingdom* 100: 1135-1146. <https://doi.org/10.1017/S0025315420001022>
- Ben Ltaief T, Drira Z, Hannachi I, Bel Hassen M, Hamza A et al. (2015). What are the factors leading to the success of small planktonic copepods in the Gulf of Gabes, Tunisia? *Journal of the Marine Biological Association of the United Kingdom* 1-15. <https://doi.org/10.1017/S0025315414001507>
- Ben Mohamed S, Mejri M, Chalh A, Shahin AAB, Quignard J-P et al. (2023). Distinct inter and intrapopulation variation in the otolith shape and size of *Mullus barbatus* (Actinopterygii: Mullidae) from the Bizerte and Ghar El Melh lagoons in Tunisian waters, *Marine Biology Research*. <https://doi.org/10.1080/17451000.2023.2203503>
- Ben-Tuvia A (1986). Mugilidae. In: Whitehead PJP, Bauchot M-L, Hureau J-C, Nielsen J, Tortonese E (editors). *Fishes of the North-eastern Atlantic and Mediterranean*. Vol. 3. Paris: UNESCO, pp. 1197-1204.
- Bose A, Adragna J, Balshine S (2017). Otolith morphology varies between populations, sexes, and male alternative reproductive tactics in a vocal toadfish *Porichthys notatus*. *Journal of Fish Biology* 90: 311-325. <https://doi.org/10.1111/jfb.13187>
- Bostanci D, Polat N, Kurucu G, Yedier S, Konaş S et al. (2015). Using otolith shape and morphometry to identify four *Alburnus* species (*A. chalcoides*, *A. escherichii*, *A. mossulensis* and *A. tarichi*) in Turkish inland waters. *Journal of Applied Ichthyology* 31 (6): 1013-1022. <https://doi.org/10.1111/jai.12860>
- Bostanci D, Yedier S (2018). Discrimination of invasive fish *Atherina boyeri* (Pisces: Atherinidae) populations by evaluating the performance of otolith morphometrics in several lentic habitats. *Fresenius Environmental Bulletin* 27 (6): 4493-4501.
- Bostancı D, Türker D, Yedier S, Konaş S, Kurucu G (2018). Investigating the fluctuating asymmetry in the otolith characters of Mediterranean horse mackerel, *Trachurus mediterraneus* (Steindachner 1868) Inhabiting Edremit Bay, North Aegean Sea. *Ordu University Journal of Science and Technology* 8 (1): 69-78.
- Bouriga N, Mejri M, Dekhil M, Bejaoui S, Quignard J-P et al. (2021). Investigating otolith mass asymmetry in six benthic and pelagic fish species (Actinopterygii) from the Gulf of Tunis. *Acta Ichthyologica et Piscatoria* 51 (2): 193-197. <https://doi.org/10.3897/aiep.51.64220>
- Bret, MT, Müller-Navarra DC (1997). The role of highly unsaturated fatty acids in aquatic food web processes. *Freshwater Biology* 13: 1055-1063. <https://doi.org/10.1046/J.1365-2427.1997.00220.X>
- Campana SE, Neilson JD (1985). Microstructure of fish otoliths. *Canadian Journal of Fisheries and Aquatic Sciences* 42: 1014-1032. <https://doi.org/10.1139/f85-127>
- Capoccioni F, Costa C, Aguzzi J, Menesatti P, Lombarte A et al. (2011). Ontogenetic and environmental effects on otolith shape variability in three Mediterranean European eel (*Anguilla anguilla*, L.) local stocks. *Journal of Experimental Marine Biology and Ecology* 397: 1-7. <http://dx.doi.org/10.1016/j.jembe.2010.11.011>
- Çöl O, Yılmaz S. (2022). The effect of ontogenetic diet shifts on sagittal otolith shape of European perch, *Perca fluviatilis* (Actinopterygii: Percidae) from Lake Ladik, Turkey. *Turkish Journal of Zoology* 46 (4): 385-396. <https://doi.org/10.55730/1300-0179.3090>
- Carvalho B, Volpedo AV, Albuquerque CQ, Favaro LF (2019). First record of anomalous otoliths of *Menticirrhus americanus* in the South Atlantic. *Journal of Applied Ichthyology* 35 (6): 1286-1291. <http://dx.doi.org/10.1111/JAI.13979>
- Carvalho B, Pérez J, Aguilar-Perera A, Noh Quiñones V, Tomás A et al. (2022). Inferring ecological connectivity between populations of *Opsanus beta* (Goode & Bean, 1880) from the southern Gulf of Mexico and the South-western Atlantic coast. *Journal of the Marine Biological Association of the United Kingdom* 102 (8): 597-603. <https://doi.org/10.1017/S0025315422000935>
- De Carvalho Lapuch, I, Carvalho BMD, Baptista-Metri C (2022). First record of anomalous otoliths in *Atherinella brasiliensis*. *Journal of Applied Ichthyology* 38 (1): 109-113. <http://dx.doi.org/10.1111/jai.14255>
- Degens ET, Deuser WG, Haedrich RL (1969). Molecular structure and composition of fish otoliths. *Marine Biology* 2: 105-113. <https://doi.org/10.1007/BF00347005>
- D'Iglio C, Albano M, Famulari S, Savoca S, Panarello G et al. (2021). Intra- and interspecific variability among congeneric *Pagellus* otoliths. *Scientific Reports* 11: 16315. <https://doi.org/10.1038/s41598-021-95814-w>
- El Kateb A, Stalder C, RuËggeberg A, Neururer C, Spangenberg JE et al. (2018). Impact of industrial phosphate waste discharge on the marine environment in the Gulf of Gabes (Tunisia). *PLoS One* 13: e0197731. <https://doi.org/10.1371/journal.pone.0197731>
- Espino-Barr E, Gallardo-Cabello M, Cabral-Solís EG, Puente-Gómez M, García-Boa A (2013). Otoliths analysis of *Mugil curema* (Pisces: Mugilidae) in Cuyutlan Lagoon, Mexico. *Avances en Investigación Agropecuaria* 17: 35-64.
- Fashandi A, Valinassab T, Kaymaram F, Fatemi SMR (2019). Morphometric parameters of the sagitta otolith among four carangids species in the Persian Gulf. *Iranian Journal of Fisheries Sciences* 18: 547-561. <https://doi.org/10.22092/ijfs.2018.116983>
- Fatnassi M, Khedher M, Trojette M, El Houda Mahouachi N, Chalh A et al. (2017). Biometric data and contour shape to assess sexual dimorphism and symmetry of the otolith pairs of *Trachinus draco* from North Tunisia. *Cahiers de Biologie Marine* 58: 261-268. <https://doi.org/10.21411/CBM.A.8EB74E07>
- Filiz H, Toğulga M (2009). Age and growth, reproduction and diet of the black goby, (*Gobius niger*) from Aegean Sea, Turkey. *Journal of Fisheries Sciences*.com 3 (3): 243-265. <http://dx.doi.org/10.3153/jfscm.2009030>

- Georgieva Y, Daskalov G, Klayn S, Stefanova K, Stefanova ES (2019). Seasonal diet and feeding strategy of horse mackerel *Trachurus mediterraneus* (Steindachner, 1868) (Perciformes: Carangidae) in the south-western Black Sea. *Acta Zoologica Bulgarica* 71: 201-210.
- Gonçalves RM, Petenuci ME, Maistrovicz FC, Galuch MB, Montanher PF et al. (2021). Lipid profile and fatty acid composition of marine fish species from Northeast coast of Brazil. *Journal of Food Science and Technology* 58 (3): 1177-1189. <http://dx.doi.org/10.1007/s13197-020-04631-y>
- Govind CK, Pearce J (1986). Differential reflex activity determines claw and closer muscle asymmetry in developing lobsters. *Science* 233 (4761): 354-356. <https://doi.org/10.1126/science.233.4761.354>
- Grønkvær P (2016). Otoliths as individual indicators: a reappraisal of the link between fish physiology and otolith characteristics. *Marine and Freshwater Research* 67: 881-888. <http://dx.doi.org/10.1071/MF15155>
- Horrocks LA, Akhlaq AF (2004). Docosahexaenoic acid in the diet: its importance in maintenance and restoration of neural membrane function. *Prostaglandins, Leukotrienes and Essential Fatty Acids* 70 (4): 361-372. <https://doi.org/10.1016/j.plefa.2003.12.011>
- Iwata H, Ukai Y (2002). SHAPE: a computer program package for quantitative evaluation of biological shapes based on elliptic Fourier descriptors. *Journal of Heredity* 93 (5): 384-385. <https://doi.org/10.1093/jhered/93.5.384>
- Jawad LA, Qasim A, Farrag M, Osman A, Samy-Kamal M et al. (2023). Investigation of otolith asymmetry in *Mulloidichthys flavolineatus* and *Parupeneus forsskali* (Perciformes: Mullidae) from Egypt's Hurgada fishing harbour on the Red Sea. *Oceanological and Hydrobiological Studies* 52 (1): 68-78. <https://doi.org/10.26881/oahs-2023.1.05>
- Joyeux JC, Bouchereau JL, Tomasini JA (1991a). La reproduction de *Gobius niger* (Pisces, Gobiidae) dans la lagune de Mauguio. France *Rapports gonadosomatiques, fécondités, ponte, oeufs et larves. Vie Milieu* 41 (2/3): 97-106.
- Joyeux JC, Tomasini JA, Bouchereau JL (1991b). Le régime alimentaire de *Gobius niger* Linné, 1758 (Teleostei, Gobiidae) dans la lagune de Mauguio, France. *Annales des Sciences Naturelles Zoologie* 13e Série 12: 57-69.
- Kara MH, Quignard J-P (2019). *Fishes in lagoons and estuaries in the Mediterranean 2, sedentary fish*. London, UK: Wiley.
- Kelly JR, Scheibling RE (2012). Fatty acids as dietary tracers in benthic food webs. *Marine Ecology Progress Series* 446: 1-22. <https://doi.org/10.3354/meps09559>
- Khedher M, Ben Faleh A, Fatnassi M, Rebaya M, Chalh A, et al. (2017). Local variability in the sagittae otolith shape of *Mugil cephalus* from the sea of Tabarka and the Dam of Nebeur in Tunisia. *Journal of Zoological Sciences* 5: 68-79.
- Khedher M, Mejri M, Shahin AAB, Quignanrd J-P, Trabelsi M et al. (2021). Discrimination of *Diplodus vulgaris* (Actinopterygii, Sparidae) stock from two Tunisian lagoons using the otolith shape analysis. *Journal of the Marine Biological Association of the United Kingdom* 101: 743-751. <https://doi.org/10.1017/S0025315421000667>
- Khemiri S, Labonne M, Gaamour A, Munaron J-M, Morize E (2014). The use of otolith chemistry to determine stock structure of *Sardina pilchardus* and *Engraulis encrasicolus* in Tunisian Coasts. *Cahiers de Biologie Marine* 55: 21-29.
- Lepage G, Roy CC (1984). Improved recovery of fatty acid through direct transesterification without prior extraction or purification. *Journal of Lipid Research* 25 (12): 1391-1396.
- Lombarte A, Palmer M, Matallanas J, Gómez-Zurita J, Morales-Nin B (2010). Ecomorphological trends and phylogenetic inertia of otolith sagittae in Nototheniidae.
- Environmental Biology of Fishes* 89: 607-618. <https://doi.org/10.1007/s10641-010-9673-2>
- Lychakov DV, Rebane YT (1993). Effect of otolith shape on directional sound perception in fish. *Journal of Evolutionary Biochemistry and Physiology* 28 (6): 707-714.
- Lychakov DV, Rebane TY, Lombarte A, Demestre M, Fuiman L (2008). Saccular otolith mass asymmetry in adult flatfishes. *Journal of Fish Biology* 72: 2579-2594. <https://doi.org/10.1111/j.1095-8649.2008.01869.x>
- Mahé K, Gourtay C, Defruit G, Chantre C, de Pontual H et al. (2019). Do environmental conditions (temperature and food composition) affect otolith shape during fish early-juvenile phase? An experimental approach applied to European Seabass (*Dicentrarchus labrax*). *Journal of Experimental Marine Biology and Ecology* 521: e151239. <https://doi.org/10.1093/icesjms/fsy163>
- Mahé K, MacKenzie K, Ider D, Massaro A, Hamed O et al. (2021). Directional bilateral asymmetry in fish otolith: a potential tool to evaluate stock boundaries? *Symmetry* 13: 987. <https://doi.org/10.3390/sym13060987>
- Marmo F (1982). Development, structure and composition of the otoliths in vertebrates. *Basic and Applied Histochemistry* 26 (2): 117-30.
- Miller JA, Wells BK, Sogard SM, Grimes CB, Cailliet GM (2010). Introduction to proceedings of the 4th International Otolith Symposium. *Environmental Biology of Fishes* 89: 203-207. <https://doi.org/10.1007/s10641-010-9715-9>
- Mejri M, Bakkari W, Allagui F, Rebaya M, Jmil I et al. (2022a). Interspecific and intersexual variability of the sagitta otolith shape between *Liza aurata* and *Chelon ramada* (Mugiliformes: Mugilidae) inhabiting the Boughrara lagoon, Tunisia. *Thalassas: An International Journal of Marine Sciences* 38: 1357-1369. <https://doi.org/10.1007/s41208-022-00460-2>
- Mejri M, Bakkari W, Tazarki M, Mili S, Chalh A et al. (2022b). Discriminant geographic variation of saccular otolith shape and size in the common Pandora, *Pagellus erythrinus* (Sparidae) across the Gulf of Gabes, Tunisia. *Journal of Ichthyology* 62 (6): 1053-1066. <https://doi.org/10.1134/S0032945222060169>
- Mille T. (2015). Sources de variation intra-populationnelle de la morphologie des otolithes: Asymétrie directionnelle et régime alimentaire. Thèse de doctorat, Université de LILLE, France (in French).

- Mille T, Mahe K, Villanueva MC, DePontual H, Ernande B (2015). Sagittal otolith morphogenesis asymmetry in marine fishes. *Journal of Fish Biology* 87: 646-663. <http://dx.doi.org/10.1111/jfb.12746>
- Mille T, Mahé K, Cachera M, Villanueva CM, De Pontual H et al. (2016). Diet is correlated with otolith shape in marine fish. *Marine Ecology Progress Series* 555: 167-184. <https://doi.org/10.3354/meps11784>
- Morte S, Redon MJ, Sanz-Brau A (1999). Feeding habits of *Trachinus draco* of the eastern coast of Spain (western Mediterranean). *Vie et Milieu* 49: 287-291.
- Munday PL, Hernaman V, Dixson DL, Thorrold SR (2011). Effect of ocean acidification on otolith development in larvae of a tropical marine fish. *Biogeosciences Discussions* 8: 2329-2356. <https://doi.org/10.5194/bgd-8-2329-2011>
- Nemova NN, Nefyodova ZA, Murzina SA (2014). Lipid patterns early in Atlantic salmon, *Salmo salar* L., ontogeny. *Transactions of KarRC RAS* 5: 44-52.
- Özbilgin H, Tosunoğlu Z, Bilecenoglu M, Tokaç A (2004). Population parameters of *Mullus barbatus* in İzmir Bay (Aegean Sea), using length frequency analysis. *Journal of Applied Ichthyology* 20 (4): 231-233.
- Díaz-Gil C, Palmer M, Catalán IA, Alós J, Fuiman LA et al. (2015). Otolith fluctuating asymmetry: a misconception of its biological relevance? *ICES Journal of Marine Science*, 72 (7): 2079-2089. <https://doi.org/10.1093/icesjms/fsy163>
- Palmer AR, Strobeck C (1986). Fluctuating asymmetry: measurement, analysis, patterns. *Annual Review of Ecology and Systematics* 17: 391-421. <http://dx.doi.org/10.1146/annurev.es.17.110186.002135>
- Panfili J, Durand J-D, Diop K, Gourene B, Simier M (2005). Fluctuating asymmetry in fish otoliths and heterozygosity in stressful estuarine environments (West Africa). *Marine and Freshwater Research* 56: 505-516. <https://doi.org/10.1071/MF04138>
- Paxton JR (2000). Fish otoliths: do sizes correlate with taxonomic group, habitat and/or luminescence? Fish Section, Sydney, Australia: Australian Museum, 6 College Street.
- Qasim A, Jawad LA, Waryani B (2022). Bilateral asymmetry in otolith size of *Pampus argenteus* (Osteichthyes: Stromatidae) from Iraqi marine waters. *Croatian Journal of Fisheries* 80 (3): 103-112. <https://doi.org/10.2478/cjf-2022-0011>
- Ramcharitar JU, Deng XH, Ketten D, Popper AN (2004). Form and function in the unique inner ear of a teleost: the silver perch (*Bairdiella chrysoura*). *Journal of Comparative Neurology* 475: 531-539. <https://doi.org/10.1002/cne.20192>
- Riede K (2004). Global register of migratory species- from global to regional scales. Final Report of the R and D-Projekt 808 05 081. Bonn, Germany: Federal Agency for Nature Conservation.
- Roux C (1990). *Trachinidae*. In: Quero JC, Hureau JC, Karrer C, Post A, Saldanha L (editors). Check-list of the fishes of the eastern tropical Atlantic (CLOFETA). Vol. 2. Lisbon, SEI, Paris: JNICT, UNESCO, pp. 893-895.
- Sargent JR, McEvoy L, Estevez A, Bell JG, Bell MV et al. (1999). Lipid nutrition of marine fish during early development: current status and future directions. *Aquaculture* 179: 217-229. [http://dx.doi.org/10.1016/S0044-8486\(99\)00191-X](http://dx.doi.org/10.1016/S0044-8486(99)00191-X)
- Shulman GE, Jakovleva KK (1983). Hexanoic acid and natural mobility of fish. *Biology Bulletin Reviews* 44: 529-540.
- Shulman GE, Yuneva TV (1990). The role of docosahexaenoic acid in adaptations fishes. *Gidrobiologicheskii Zhurnal* 26: 43-51.
- Škeljo F, Brčić J, Vuletin V, Ferri J (2015). Age and growth of the axillary wrasse, *Symphodus mediterraneus* (L.) from the eastern Adriatic Sea. *Marine Biology Research* 11: 780-784. <https://dx.doi.org/10.1080/17451000.2015.1016963>
- Smith WE, Kwak TJ (2014). A capture-recapture model of amphidromous fish dispersal. *Journal of Fish Biology* 84: 897-912. <https://doi.org/10.1111/jfb.12316>
- Sonin O, Spanier E, Levi D, Patti B, Rizzo P et al. (2007). Nanism (dwarfism) in fish: a comparison between red mullet *Mullus barbatus* from the southeastern and the central Mediterranean. *Marine Ecology Progress Series* 343: 221-228. <https://dx.doi.org/10.3354/meps06917>
- Stanley RRE, Bradbury IR, DiBacco C, Snelgrove PVR, Thorrold SR et al. (2015). Environmentally mediated trends in otolith composition of juvenile Atlantic cod (*Gadus morhua*). *ICES Journal of Marine Science* 72: 2350-2363. <https://doi.org/10.1093/ICESJMS/FSV070>
- Storelli MM, Giacomini R, Marcotrigiano GO (1998). Total mercury in muscle of benthic and pelagic fish from the South Adriatic Sea (Italy). *Food Additives and Contaminants* 15 (8): 876-883. <https://doi.org/10.1080/02652039809374724>
- Suthers IM (1996). Spatial variability of recent otolith growth and RNA indices in pelagic juvenile *Diaphus kapalae* (Myctophidae): an effect of flow disturbance near an island? *Marine and Freshwater Research* 47 (2): 273-282. <https://doi.org/10.1071/MF9960273>
- Thomson JM (1990). *Mugilidae*. In: Quero JC, Hureau JC, Karrer C, Post A, Saldanha L (editors). Check-list of the fishes of the eastern tropical Atlantic (CLOFETA). Vol. 2. Lisbon, SEI, Paris: JNICT, UNESCO, pp. 855-859.
- Toğulga M (1977). The studies on population dynamics of red mullet (*Mullus barbatus* Lin. 1758) in İzmir Bay. Ege University, *Journal of Faculty of Science Series B* 2: 175-194.
- Trojette M, Ben Faleh A, Fatnassi M, Marsaoui B, Mahouachi N et al. (2015). Stock discrimination of two insular populations of *Diplodus annularis* (Actinopterygii: Perciformes: Sparidae) along the coast of Tunisia by analysis of otolith shape. *Acta Ichthyologica et Piscatoria* 45 (4): 363-372. <http://dx.doi.org/10.3750/AIP2015.45.4.04>
- Tserpes G, Fiorentino F, Levi D, Cau A, Murenu M et al. (2002). Distribution of *Mullus barbatus* and *M. surmuletus* (Osteichthyes: Perciformes) in the Mediterranean continental shelf: implications for management. *Scientia Marina* 66: 39-54.

- Tuset VM, Jurado-Ruzafa A, Otero-Ferrer JL, Santamaría MTG (2019). Otolith phenotypic variability of the blue jack mackerel, *Trachurus picturatus*, from the Canary Islands (NE Atlantic): implications in its population dynamic. *Fisheries Research* 218: 48-58. <http://dx.doi.org/10.1016/j.fishres.2019.04.016>
- Tuset VM, Lombarte A, Bariche M, Maynou F, Azzurro E (2020). Otolith morphological divergences of successful Lessepsian fishes on the Mediterranean coastal waters. *Estuarine, Coastal and Shelf Science* 236: 106631. <https://doi.org/10.1016/j.ecss.2020.106631>
- van der Lingen C, Bertrand A, Bode A, Brodeur R, Cubillos LA (2009). Trophic dynamics. In: Checkley DM, Alheit J, Oozeki Y, Roy C (editors). *Climate change and small pelagic fish*. Cambridge: Cambridge University Press, pp. 112-157.
- Vasconcelos J, Vieira AR, Sequeira V, González JA, Kaufmann M et al. (2018). Identifying populations of the blue jack mackerel (*Trachurus picturatus*) in the Northeast Atlantic by using geometric morphometrics and otolith shape analysis. *Fisheries Bulletin* 116: 81-92. <http://dx.doi.org/10.7755/FB.116.1.9>
- Vignon M, Morat F (2010). Environmental and genetic determinant of otolith shape revealed by a non-indigenous tropical fish. *Marine Ecology Progress Series* 411: 231-241. <http://dx.doi.org/10.3354/meps08651>
- Voronin VP, Nemova NN, Ruokolainen TR, Artemenkov DV, Rolskii AY et al. (2021). Into the deep: New data on the lipid and fatty acid profile of redfish *Sebastes mentella* inhabiting different depths in the Irminger Sea. *Biomolecules* 11: 704. <https://doi.org/10.3390/biom11050704>
- Yazici R (2023). Sex-linked variations in the sagittal otolith biometry of *Nemipterus randalli* (Russell, 1986) from the eastern Mediterranean Sea. *Journal of Fish Biology* 102 (1): 241-247. <https://doi.org/10.1111/jfb.15256>
- Yedier S (2022). First record of abnormal otoliths in the greater weever *Trachinus draco* (Trachinidae) in the Black Sea. *Journal of Ichthyology* 62 (5): 760-769. <https://doi.org/10.1134/S0032945222050253>
- Yedier S, Bostanci D (2019). Aberrant crystallization of blackbellied angler *Lophius budegassa* Spinola, 1807 otoliths. *Cahiers de Biologie Marine* 60 (6): 527-533. <http://dx.doi.org/10.21411/cbm.a.2389af48>
- Yedier S, Bostanci D (2020). Aberrant otoliths in four marine fishes from the Aegean Sea, Black Sea, and Sea of Marmara (Turkey). *Regional Studies in Marine Science* 34: 1-7. <http://dx.doi.org/10.1016/j.rsma.2019.101011>
- Yedier S, Bostanci D (2021). Morphologic and morphometric comparisons of sagittal otoliths of five *Scorpaena* species in the Sea of Marmara, Mediterranean Sea, Aegean Sea and Black Sea. *Cahiers de Biologie Marine* 62 (4): 357-369. <https://doi.org/10.21411/CBM.A.6B8915B2>
- Yedier S, Bostanci D (2022). Molecular and otolith shape analyses of *Scorpaena* spp. in the Turkish seas. *Turkish Journal of Zoology* 46 (1): 78-92. <https://doi.org/10.3906/zoo-2105-26>
- Yedier S, Konaş S, Bostanci D (2022). Assessing of fluctuating asymmetry in otolith of the *Alburnus* spp. from Anatolian lotic and lentic systems. *Ege Journal of Fisheries and Aquatic Sciences* 39 (1): 32-38. <http://dx.doi.org/10.12714/egejfas.39.1.05>
- Yedier S, Bostanci D, Türker D (2023). Morphological and morphometric features of the abnormal and normal saccular otoliths in flatfishes. *The Anatomical Record* 306 (3): 672-687. <https://doi.org/10.1002/ar.25106>
- Zaoui N, Bouriga N, Louiz I, Bahri WR, Saadaoui N et al. (2023). Assessment of effects of metal contamination and abiotic factors on fatty acid composition and biochemical biomarkers activity in the liver of *Chelon ramada* collected from two ecosystems on the Mahdia coast, Tunisia. *Biochemical Systematics and Ecology* 107: 104608. <https://doi.org/10.1016/j.bse.2023.104608>
- Zhang X, Ning X, He X, Sun X, Yu X, Cheng Y et al. (2020). Fatty acid composition analyses of commercially important fish species from the Pearl River Estuary, China. *PLoS ONE* 15 (1): e0228276. <https://doi.org/10.1371/journal.pone.0228276>
- Zhang S, Zhang X, Gao S, Shu R, Fu G, Lu J (2023). Bilateral asymmetry of otoliths from *Collichthys lucidus* of different sizes in Haizhou Bay and Xiangshan Bay. *Journal of Fish Biology* 102 (2): 403-412. <https://doi.org/10.1111/jfb.15276>